The Aeronautical Journal (2026), 1–44
doi:10.1017/aer.2026.10244

RESEARCH ARTICLE

Optimizing aircraft trajectories under convective weather conditions

Zekeriya Kaplan[1], Cem Çetek[2] and Tuğba Saraç[3]

[1]Aircraft Maintenance Department, Samsun University, Samsun, Türkiye
[2]Air Traffic Control Department, Eskisehir Technical University, Türkiye
[3]Industrial Engineering Department, Eskisehir Osmangazi University, Türkiye
Corresponding author: Zekeriya Kaplan; Email: zekeriya.kaplan@samsun.edu.tr

Received: 4 February 2026 UTC; **Revised:** 25 August 2026 UTC; **Accepted:** 25 August 2026 UTC

Keywords: Air Traffic Management; Convective Weather Avoidance; Rolling Horizon Control; Stochastic Programming; Wind Uncertainties

Abstract

This study focuses on trajectory optimisation in air traffic management (ATM), addressing the challenges of flight planning under convective weather conditions. Convective weather, including hail, wind shear and severe icing, can pose significant operational risks and require aircraft to avoid these areas. Deviations from planned trajectories lead to additional flight distances, delays and operational disruptions, highlighting the need for effective trajectory planning approaches. In this study, deterministic and stochastic models were developed to optimise aircraft trajectories, with the stochastic model accounting for wind uncertainties. A rolling horizon control (RHC) approach was implemented to address the dynamic behaviour of convective areas, enhancing model realism. The models aim to minimise total flight time while maintaining conflict-free operations and avoiding convective weather areas. Results demonstrate the effect of incorporating wind uncertainty through the stochastic model on ATM performance, particularly under convective weather conditions. The proposed algorithms support decision-making and automation, enabling coordinated trajectory planning and reducing workload for pilots and air traffic controllers. This approach improves ATM safety, efficiency and capacity under adverse weather conditions.

Nomenclature

ATM	air traffic management
ATCOs	air traffic controllers
ATFM	air traffic flow management
CB	cumulonimbus
GS	ground speed
MILP	mixed-integer linear programming
MINLP	mixed-integer nonlinear programming
NLP	nonlinear programming
NMPC	nonlinear model predictive control
RHC	rolling horizon control
TAS	true airspeed
TMA	terminal manoeuvring area
TP	test problem
TS	thunderstorm
VSS	value of the stochastic solution

© The Author(s), 2026. Published by Cambridge University Press on behalf of Royal Aeronautical Society. This is an Open Access article, distributed under the terms of the Creative Commons Attribution licence (https://creativecommons.org/licenses/by/4.0/), which permits unrestricted re-use, distribution and reproduction, provided the original article is properly cited.

Downloaded from https://www.cambridge.org/core. 17 Nov 2026 at 23:48:34, subject to the Cambridge Core terms of use.

1. Introduction

1.1. Motivation

Trajectory optimisation aims to obtain cost-efficient flights and enhance overall operational efficiency. Therefore, it is a fundamental aspect of the air traffic management (ATM) system. However, convective weather areas significantly affect aircraft operations and create major challenges for aircraft trajectory planning in ATM systems. In these areas, severe weather events such as hail, wind shear, lightning, severe icing and turbulence present major safety risks to aircraft. For this reason, aircraft should avoid them to minimise the risk of encountering severe weather events. Hence, an effective flight trajectory planning algorithm is crucial in ATM, as it can help aircraft avoid these events.

Avoiding convective weather leads to deviations from planned flight plans, which cause air traffic disruptions when multiple flights are affected simultaneously. Such disruptions will increase flight time and delay, resulting in congestion and additional fuel consumption within the airspace [1]. Delays occur due to convective weather, which introduces challenges in predicting air traffic and adds complexity to its management. Additionally, the workload of the flight crew increases significantly due to decision-making, turbulence, icing management and increased communications. Similarly, air traffic controllers (ATCOs) experience a substantial workload increase during convective weather, mainly due to irregular air traffic and less available airspace. These factors reduce the airspace capacity, consequently negatively affecting flight efficiency. Furthermore, the inherent uncertainty of convective weather and its impact on airspace capacity require advanced safety measures and automated flight routeing systems.

Convective weather conditions remain a major contributor to delays in European air traffic flow management (ATFM). Approximately 4 million minutes of delay per year are attributed to convective weather conditions during en-route flights [2]. In July 2023, Europe experienced convective weather conditions, including thunderstorms. EUROCONTROL reported that the weather-related ATFM delay for this month exceeded two and a half times that of the previous year. When excluding weather-related factors, ATFM delays per flight decreased by almost a quarter despite a 7% increase in air traffic. However, when considering the impact of convective weather, delays increased slightly from 3.9 to 4.1 min per flight [3]. This indicates that convective weather contributes to air traffic delays, highlighting the need for improved strategies to mitigate its operational impact and enhance flight efficiency. Therefore, EUROCONTROL initiated the SMART Weather Task Force programme to enable collaborative management of convective weather conditions [4].

Convective weather events are also impacted by climate change. As global temperatures rise, changes in atmospheric conditions influence convective weather phenomena like thunderstorms, tornadoes and heavy rainfall. However, it is important to note that these effects can vary depending on regional and local atmospheric conditions. Some studies and researchers have examined the impact of global warming on weather phenomena, including thunderstorms, and have noted that some regions may experience frequent and intense convective weather events while others may see different climate changes [5–8].

In addition to the challenge of avoiding convective weather conditions, potential conflicts between aircraft within the airspace represent another critical operational challenge. When pilots encounter convective weather along planned flight trajectories, they promptly notify ATCOs to determine the appropriate avoidance manoeuvres using weather radar. Multiple pilots within the same airspace may make similar requests, leading to potential conflicts as aircraft deviate from their flight trajectories. ATCOs are responsible for resolving these potential conflicts and providing necessary instructions to maintain safe air traffic flow by ensuring conflict-free flight trajectories. However, there is less available area in the airspace to resolve conflicts due to convective weather conditions, adding an extra complexity to ATM with irregular air traffic and increasing congestion. As airspace congestion continues to rise, the workload of ATCOs increases significantly. To address this, developing algorithms that propose conflict-free trajectories under convective weather conditions is essential. Decision support and/or automation systems based on these algorithms can be effective tools for improving the accuracy and efficiency of aircraft trajectory planning and coordination within the airspace. As a result, the use of

Downloaded from https://www.cambridge.org/core. 17 Nov 2026 at 23:48:34, subject to the Cambridge Core terms of use.

these algorithms can help reduce ATCO workload, with potential benefits for operational safety and ATM capacity.

Some avoidance guidelines have been presented by authorities that describe what pilots should do to continue their flights safely in case of encountering convective areas [9–12]. However, Reference [13] has shown that these guidelines are inadequate and overly simplify the hazardous turbulence conditions surrounding convective areas. Because the decision-making processes of pilots regarding weather conditions are highly complex and dynamic, pilots make decisions based on their own experience and real-time observations of weather information, along with information obtained from remotely sensed data and observed flight trajectories [14]. Moreover, although some meteorological conditions can be predicted in advance, it is difficult to determine the specific location and time of convective weather. Therefore, convective weather forecasting and avoidance primarily occur during the flight at short timescales. The approach proposed in our study can guide pilots and ATCOs based on real-time observations through onboard weather radar of convective areas, along with indicators.

This study develops mathematical models to optimise aircraft trajectories in ATMs under convective weather conditions, specifically focusing on the dual challenges of avoiding convective areas and resolving conflicts between aircraft during en-route flights. This approach not only contributes to the theoretical foundation but also addresses practical applications in enhancing flight safety and efficiency. To achieve this, we have proposed two distinct models, one utilising a deterministic approach and the other employing stochastic programming that considers the uncertainties of both wind direction and speed. The objective of these models is to minimise the total flight time of the aircraft while determining flight trajectories between the entry and exit points of the airspace under convective weather conditions. Moreover, we have implemented a rolling horizon control (RHC) approach to address the dynamic nature of convective areas. This framework allows us to address changes in the size and displacement of the convective areas over time, including merging, splitting, dissipating and growing behaviour, thereby enhancing the effectiveness of models in optimising flight paths.

1.2. Literature review

There are studies in the literature that detect and resolve potential conflicts between aircraft during the en-route phase of flights. These studies aimed to explore effective conflict resolution techniques, manoeuvre strategies and solution approaches to ensure the safe and efficient management of airspace. Researchers have introduced several mathematical models, including mixed-integer linear programming (MILP) and mixed-integer nonlinear programming (MINLP), as well as heuristic and metaheuristic algorithms. These models and algorithms utilise airspace discretisation and geometric structure-based discretisation techniques to deal with conflict resolution.

Cecen and Cetek [15] resolved potential conflicts between aircraft using entry point assignment and speed change manoeuvres, while in another study Reference [16], employed entry point assignment and heading change manoeuvres for conflict resolution. Additionally, Reference [17] addressed conflicts involving changes in heading and altitude. In all three studies, the authors utilised the airspace discretisation technique and assumed conflict resolution manoeuvres would take place within a predefined buffer zone within the boundaries of the airspace. Together with the mathematical model, they proposed using heuristic and metaheuristic algorithms for the problem solution, including simulated annealing and tabu search. Some researchers [18–21] have also used the airspace discretisation technique to resolve conflicts without defining any buffer zone within the airspace. These studies have introduced a mathematical model, with the first study by Reference [18] also proposing a heuristic algorithm.

In addition to the studies mentioned above, several studies have been conducted on mathematical models based on the geometric structure approach. In the study by Reference [22], only the speed change manoeuvre was used to resolve conflicts between aircraft, while in the study by Reference [23], only the heading change manoeuvre was used. However, in some studies [24–27], both heading and speed change manoeuvres were used. Additionally, studies [28, 29] were conducted using both altitude and speed change manoeuvres. All three manoeuvres were used in the study [30]. On the other hand, solutions were

Downloaded from https://www.cambridge.org/core. 17 Nov 2026 at 23:48:34, subject to the Cambridge Core terms of use.

produced using the heuristic algorithm [31] and the particle swarm optimisation metaheuristic algorithm [32]. In the first study, only heading change was used, while in the second study, both heading and speed change manoeuvres were used. The number of nodes used to discretise the airspace affects the solution time and quality of the model. A higher number of nodes leads to better solutions, but it also increases the solution time in both airspace discretisation and geometric structure-based approaches. Reference [33] presented a mathematical model to solve conflicts between aircraft. In their study, the airspace was discretised into low, medium and high node numbers to examine the effect of the discretisation rate on the solution time and quality.

Recent studies on aircraft trajectory optimisation have explored diverse methodological approaches to address operational, environmental and uncertainty-related challenges in ATM. Several studies have developed robust frameworks to consider weather-related uncertainties in trajectory planning. NG (2022) [34] developed a robust flight path planning approach that accounts for fuel and contrail costs under meteorological uncertainty. The method models airspace as a directed graph, identifying contrail-prone regions from temperature and humidity thresholds. Using an adjustable robust optimisation framework with Benders decomposition, the approach balances environmental impact and operational efficiency.

Kamo et al. [35] developed an integrated optimisation framework that jointly determines aircraft trajectories and arrival sequences under meteorological forecast uncertainty. The approach combines robust optimal control and MINLP to optimise 4D trajectories while maintaining safe separation and improving throughput and fuel efficiency. Ensemble weather forecasts are used to model uncertainty, and performance surfaces are introduced to link sequencing and trajectory decisions. Computational efficiency is achieved by relaxing the MINLP into an equivalent nonlinear programming (NLP). A related study by Reference [36] focuses on multi-aircraft 4D trajectory planning in terminal manoeuvring area (TMA) operations under evolving multi-cell storms. Their approach employs a receding horizon framework combined with nonlinear model predictive control (NMPC) to dynamically update aircraft trajectories as storm cells develop. Convective areas are represented as moving ellipsoids, and embedding techniques are used to transform disjunctive constraints into continuous forms, enabling efficient optimisation. The method effectively resolves conflicts and maintains safe separation in highly dynamic weather.

The optimisation of aircraft trajectories under convective weather conditions presents a significant challenge in ATMs, requiring the integration of advanced modelling techniques to ensure flight safety and efficiency. The approaches and methodologies presented in the literature to address the challenges posed by convective weather and conflict resolution between aircraft, with a particular emphasis on optimising aircraft trajectories, have been examined.

Some research into trajectory optimisation under convective weather conditions primarily focused on single-aircraft operation. Hauf et al. [37] investigated trajectory optimisation through a geometric airspace structure, applying the DIVMET method to avoid convective weather without considering the variabilities introduced by the wind. The authors described how DIVMET incorporates both static and dynamic weather conditions, requiring continuous adjustments to the navigation strategy. They utilise radar-based storm data, updated every five min, and employ a space-time interpolation technique between updates to ensure a smoother and more consistent delivery of weather information as needed. Several studies [38–40] presented various algorithmic approaches, including heuristic and reach-avoid algorithms, to avoid convective weather conditions. The first study considered convective weather conditions to be dynamic, assuming access to real-time weather data transmitted to the aircraft. Unlike the first study, the second one considered convective weather as static, even though it involved weather forecasting and updates. The third study compares two storm management strategies for flight planning: stochastic reachability, viewing storms as random obstacles in discrete time, and robust optimal control, modelling storm dynamics in continuous time. Andrés et al. [41] proposed a heuristic method for single-aircraft trajectory planning under convective weather uncertainty by combining ensemble thunderstorm forecasts with a dynamic graph-based framework. In their approach, the airspace is modelled as a directed graph, where convective regions are represented as dynamically changing forbidden zones based on ensemble predictions. The method employs an iterative graph deformation algorithm with an Augmented Random Search (ARS) heuristic to progressively refine feasible routes, ensuring avoidance

Downloaded from https://www.cambridge.org/core. 17 Nov 2026 at 23:48:34, subject to the Cambridge Core terms of use.

of hazardous weather. However, a common limitation among these studies is the neglect of wind effects and conflict resolution between multiple aircraft, which are crucial for real-world applications. Despite their innovative approaches to convective weather avoidance, each of these studies fails to address the significant impact that wind can have on the accuracy of trajectory planning and the safe separation between aircraft.

Hentzen et al. [42] developed a stochastic storm model in geometric airspace, using a reach-avoid approach to address stochastic weather and to maximise the probability of reaching a waypoint while avoiding convective weather. Both the aircraft and the storms are represented using probabilistic models. On the other hand, some studies focused on uncertainties without incorporating convective weather considerations into their models. Reference [43] developed a MILP model to generate stochastic routes within structured airspace, considering wind and temperature uncertainties. Meanwhile, Reference [44] introduced the toolchain for multi-criteria aircraft trajectory optimization (TOMATO) model in the presence of uncertain wind speed and direction. TOMATO utilises the data provided by ensembles to create a three-dimensional corridor in geometric airspace configuration.

In some studies, solution approaches have been proposed to determine convective area avoidance routes for multiple aircraft, without considering the potential conflicts between aircraft. Taylor et al. [45] investigated geometric airspace accommodating multiple aircraft, using a multi-objective genetic algorithm to evaluate trade-offs between multiple criteria of operational acceptability. The routes were designed for one or more flights in the presence of convective weather areas, using a variation on Dijkstra's shortest-path algorithm. The proposed approach was tested for nine flights requiring route planning around convective weather. Pang et al. [46] also focused on geometric airspace management for multiple aircraft, proposing a Bayesian deep learning method to predict aircraft trajectories while considering weather uncertainties. The proposed methodology was validated with real flight trajectories, flight plans and convective weather data from the Sherlock database.

The complexity of the problem increases significantly when multiple aircraft are considered, as conflict resolution between aircraft is required in addition to weather avoidance. Liu and Hwang [47] addressed both aircraft–weather and aircraft–aircraft conflicts using a stochastic optimal control framework based on Markov-chain approximation. Their formulation incorporates uncertainties in aircraft and wind dynamics and considers both static and moving weather cells. For the moving-weather case, the weather cells are represented as time-dependent regions, with constant velocities used in the simulation examples. To reduce the computational complexity of aircraft–aircraft conflict resolution, a decomposition technique was introduced for conflicting aircraft pairs. However, the authors noted that the resulting centralised approach could not efficiently resolve conflicts involving a large number of aircraft. Recent research has focused on 4D trajectory planning in free-route airspace under uncertain weather conditions. This approach uses multi-module frameworks that integrate trajectory prediction, dynamic airspace configuration and strategic and tactical trajectory optimisation. These frameworks leverage ensemble weather forecasts and distribute multi-objective optimisation. This enhances safety, flexibility and efficiency while substantially reducing risk with only a minor cost increase [48]. While these approaches are effective at the strategic level, they primarily focus on managing free-route traffic and do not explicitly address trajectory optimisation in response to rapidly evolving convective weather conditions.

Some studies highlighted the various natures of convective areas – static, dynamic or stochastic – and several solution approaches for managing air traffic, including multiple aircraft. Pannequin et al. [49] presented a nonlinear model predictive control algorithm for aircraft route planning in static convective weather. This work specifically addressed the challenge of convective weather avoidance in en-route airspace. It utilised a novel approach for computing the objective function derived from the solution to the Hamilton-Jacobi equation for minimum flight time. Erzberger et al. [50] aimed at solving separation assurance problems, including separation conflicts, arrival sequencing and weather-cell avoidance, which play a crucial role in designing future ATM systems like NextGen in the United States. Their approach included integrated algorithms to handle these problems collectively, highlighting the importance of unified solutions in managing the complexities of en-route airspace. Clarke et al. [51] developed a stochastic model for determining the capacity of a volume of airspace under uncertain

Downloaded from https://www.cambridge.org/core. 17 Nov 2026 at 23:48:34, subject to the Cambridge Core terms of use.

convective weather conditions. Their framework incorporates probabilistic convective weather forecasts into airspace capacity assessment and aircraft routeing decisions. Kamgarpour et al. [52] addressed the generation of safe aircraft trajectories under dynamic convective weather conditions using forecast information and a receding horizon approach. However, these studies do not consider wind uncertainty within aircraft trajectory dynamics or trajectory optimisation.

Recent literature has further highlighted the role of meteorological information in aviation trajectory optimisation and weather-related decision support. Akdogan and Sahin [53] reviewed 57 studies published between 2001 and 2024 and emphasised the importance of wind, temperature and convective weather in trajectory optimisation. Rathnakumar and Liu [54] developed an uncertainty-aware, vision-based weather decision-support system for general aviation using onboard camera data and semantic weather descriptors.

The literature most closely related to the present study demonstrates that different aspects of aircraft routeing and conflict resolution under convective weather and weather-related uncertainty have been investigated. Pannequin et al. [49] addressed aircraft routeing under static convective weather, while [51] incorporated probabilistic convective weather information into stochastic airspace capacity and routeing decisions. Kamgarpour et al. [52] considered trajectory generation under moving convective weather using a receding horizon approach, whereas Reference [47] incorporated wind uncertainty into a stochastic optimal control framework while addressing both aircraft–weather and aircraft–aircraft conflicts. However, these studies differ substantially in the representation of wind uncertainty, the incorporation of convective weather into trajectory optimisation, and the treatment of conflicts among multiple aircraft. Table 1 summarises the main characteristics of the studies most closely related to the present work and highlights the positioning of the proposed approach.

1.3. Contribution of the research

Although previous studies have addressed various combinations of aircraft routeing, conflict resolution, convective weather and weather-related uncertainties, they have employed different modelling frameworks and representations of wind uncertainty. In particular, the literature includes approaches based on stochastic weather information, static or moving convective weather and stochastic wind dynamics. The present study differs by integrating discrete wind uncertainty, convective weather avoidance and conflict resolution for multiple aircraft within a two-stage stochastic RHC framework. Wind speed and direction are represented through discrete probabilistic wind scenarios derived from historical upper-air observations, and the resulting scenario-dependent wind conditions are incorporated directly into trajectory optimisation and conflict-resolution decisions. The framework also accounts for the temporal evolution of convective weather areas within the rolling horizon planning process, allowing aircraft trajectories to be re-optimised as the convective areas change over time. Accordingly, this study evaluates the effectiveness of stochastic modelling for trajectory planning under convective weather and uncertain wind conditions. In particular, the study evaluates whether incorporating wind uncertainty can provide flight trajectories with lower flight-time costs than those obtained from a deterministic formulation and examines the feasibility of deterministic trajectories when exposed to alternative wind conditions.

The main specifications and contributions of the stochastic model developed in this study can be summarised as follows:

- The model represents wind speed and wind direction as sources of uncertainty through a set of discrete probabilistic wind scenarios derived from historical upper-air observations.
- Under uncertain wind conditions, the model simultaneously performs conflict resolution among multiple aircraft and avoidance of convective weather areas within a unified stochastic trajectory optimisation framework.
- The proposed framework incorporates the temporal evolution of convective weather information within the rolling horizon planning process, allowing trajectories to be re-optimised as the convective areas change over time.

Downloaded from https://www.cambridge.org/core. 17 Nov 2026 at 23:48:34, subject to the Cambridge Core terms of use.

Table 1. *Summary of related literature*

Study	Airspace structure	Number of aircraft	Conflict resolution	Convective weather	Wind uncertainty	Solution method
Hauf et al. [37]	Geographical	1	No	Dynamic	No	DIVMET model
Schilke and Hecker [38]	Geographical	1	No	Dynamic	No	Heuristic algorithm
Xie and Zhong [39]	Geographical	1	No	Static	No	Heuristic algorithm
González-Arribas et al. [40]	Geographical	1	No	Stochastic	No	Reach-avoid algorithm
Hentzen et al. [42]	Geographical	1	No	Stochastic	Yes	Reach-avoid algorithm
Franco et al. [43]	Structured	1	No	No	Yes	MILP
Lindner et al. [44]	Geographical	1	No	No	Yes	TOMATO model
Andrés et al. [41]	Directed graph	1	No	Stochastic	No	ARS-based heuristic algorithm
Taylor et al. [45]	Geographical	>1	No	Static	No	Genetic algorithm
Pang et al. [46]	Geographical	>1	No	Stochastic	No	Deep learning algorithm
Liu and Hwang [47]	Geographical	>1	Yes	Static and moving	Yes	Stochastic optimal control algorithm, Markov chain
Pannequin et al. [49]	Geographical	>1	Yes	Static	No	Nonlinear algorithm, MPC
Clarke et al. [51]	Geographical	>1	Yes	Stochastic	No	Stochastic programming, RHC
Kamgarpour et al. [52]	Geographical	>1	Yes	Dynamic	No	Nonlinear algorithm, RHC
Erzberger et al. [50]	Geographical	>1	Yes	Static	No	Heuristic algorithm
Proposed models in this study	**Airspace Discretisation**	**>1**	**Yes**	**Dynamic**	**Yes**	**MILP, RHC**

- The model is formulated using a two-stage stochastic programming framework within a rolling horizon control strategy, enabling stochastic decisions to be updated as new planning horizons are considered.
- The mathematical formulation is designed to be extendable to different airspace sizes and flight levels, providing a basis for application to other airspace configurations and operational settings.

Downloaded from https://www.cambridge.org/core. 17 Nov 2026 at 23:48:34, subject to the Cambridge Core terms of use.

2. Problem statement

En-route airspace is the largest airspace segment of the flight that aircraft travel through from the end-point of a departure procedure to the start point of an arrival procedure. There are two main types of en-route airspace structures: fixed route and free route. In fixed route airspaces, pilots should follow predefined routes consisting of waypoints. In free route airspace, however, pilots can choose their flight routes between defined airspace entry and exit points using any route rather than being restricted to flying on fixed routes. This flexibility allows for more efficient routeing and optimal airspace utilisation [15].

This study addresses en-route flights in free route airspace under convective weather conditions, applying airspace discretisation. Airspace discretisation is a technique that focuses on a finite set of strategically important points in the airspace, rather than scanning the entire airspace [15]. This method reduces computational complexity by dividing the airspace into segments or critical points that are most likely to be important for trajectory planning and conflict resolution. These include airspace entry and exit points, as well as points where the trajectories of two conflicting aircraft intersect, commonly referred to as potential conflict points. By focusing on these important points along the planned flight paths, including trajectory intersections, the model can be formulated with a limited and manageable number of variables and constraints. Within this framework, separation between aircraft is maintained by ensuring sufficient time intervals between their arrivals at these conflict points [20].

In this discretised network, potential conflicts are broadly classified into two main types: crossing conflicts, and conflicts along the same route. Crossing conflicts encompass merging and diverging route geometries. To avoid crossing conflicts, the required horizontal separation distance is converted into a minimum time separation using Equation (1), which considers the aircraft airspeeds and the angle between their flight directions [20]. While this equation fundamentally assumes linear trajectories within the potential conflict region, aircraft may change direction at the intersection points. Therefore, to accurately determine the angle (θ) required to calculate the merging (sep^{mrg}) and diverging (sep^{div}) separation times, the track lines of aircraft are linearly extended beyond the crossing points, and the angle between these extended track lines is used. On the other hand, conflicts along the same route consist of trailing and head on encounters. Trailing conflicts are avoided by strictly prohibiting overtaking within the airspace segments. For head-on encounters, the separation parameter (sep^{head}) is calculated using Equation (1), with the relevant angle determined from the extended track lines and the most restrictive divergence angle scenario considered. It ensures that the aircraft entering the segment first clears the exit point by a specified time separation before the opposing aircraft arrives at the same point. Ultimately, all calculated separation times are added to the optimisation models as parameters.

$$sep = \frac{D}{v_i v_j \left|\sin\theta_{ij}\right|} \sqrt{(v_i)^2 + (v_j)^2 - 2v_i v_j \cos\theta_{ij}} \tag{1}$$

In Equation (1), sep is the minimum time separation, D is the minimum horizontal separation distance, v_i and v_j are the airspeeds of the aircraft, θ_{ij} is the route crossing angle. In the deterministic model, true airspeed (TAS) is used in the equation, whereas in the stochastic model, ground speed (GS) is used for each wind scenario.

Moreover, the application of airspace discretisation is advantageous during convective weather conditions. By identifying and isolating the grids or points, this approach allows for the dynamic routeing of aircraft around convective weather areas. Consequently, this approach allows for more effective monitoring and intervention, reducing the likelihood of conflicts and improving overall safety in the airspace. Additionally, airspace discretisation facilitates the implementation of automated conflict detection systems, enabling real-time assessment and response to potential conflicts, thus enhancing the efficiency of ATM operations.

Figure 1 shows the structure of free route airspace, including convective areas with convective weather conditions. Aircraft enter this airspace at predefined times via entry points $ep_1, ep_2, \ldots, ep_e$ and aim to reach the exit points $op_1, op_2, \ldots, op_o$ using the shortest possible routes. These routes, represented by dashed lines in the figure, show the most direct paths between entry and exit points and are known as direct routes. The intersections of these direct flight routes, where potential aircraft conflicts

Downloaded from https://www.cambridge.org/core. 17 Nov 2026 at 23:48:34, subject to the Cambridge Core terms of use.

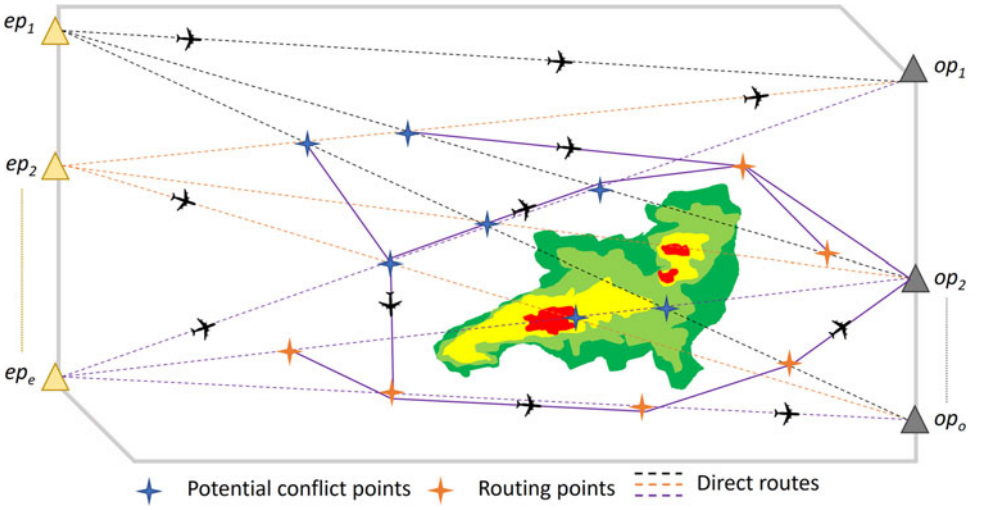


Figure 1. *Structure of free route airspace including convective areas.*

could occur, are marked with blue points. It is essential to detect and resolve potential conflicts at these points based on the arrival times of the aircraft. The figure also highlights the presence of convective weather areas, shown in various shades of green, yellow and red, indicating different levels of weather severity. They are designated as no-fly zones to prevent aircraft from entering these hazardous areas.

Turbulence is not limited to within the convective clouds but also affects the surrounding areas. Given that meteorological radars cannot detect turbulence in clear skies, convective areas should be cleared by a minimum of 20 NM laterally. If flying over a convective cloud is unavoidable, a vertical clearance of 5,000 ft is required [9]. Orange points in Figure 1 represent waypoints used for routeing around convective areas. The purple lines indicate possible routes that incorporate these waypoints. Using the airspace discretisation technique and focusing on these critical points enables the ATM system to monitor and manage air traffic flow more efficiently, thereby ensuring safety and efficiency even during convective weather conditions.

In this study, operations are considered at a single flight level. ATCOs continuously monitor traffic, and when they detect a potential conflict, they design manoeuvres that involve changes in speed, heading, or altitude. However, altitude changes are rare due to factors such as passenger comfort, increased fuel consumption and the complexity of monitoring vertical movements [20]. Pilots generally prefer horizontal manoeuvres to save fuel and time, provide more flexibility and improve safety [37]. Additionally, changing altitude may not effectively avoid convective weather areas, which can extend vertically through multiple flight levels. In busy airspace, altitude changes can create conflicts with other aircraft, complicating traffic management [52]. Thus, maintaining a single flight level simplifies trajectory optimisation, improving safety and efficiency under convective weather conditions.

A section of airspace measuring $120 \times 120\,\text{nm}^2$, as shown in Figure 2, is examined to optimise aircraft trajectories by implementing airspace discretisation techniques. The 120×120 NM airspace was selected to provide sufficient spatial extent for representing alternative trajectories around convective areas while maintaining a computationally tractable optimisation problem. This airspace is composed of 41 points, including three airspace entry points (ep_1, ep_2, ep_3) and three airspace exit points (op_1, op_2, op_3). The number of waypoints, also referred to as the discretisation rate, was determined based on a trade-off between computational efficiency and solution quality in terms of total flight time. The selection of fewer points would reduce the solution time but could result in lower solution quality. Conversely, increasing the number of points beyond a certain threshold produces relatively small improvements in trajectory optimisation, while causing an exponential increase in solution time. As shown by Reference [33], using a balanced discretisation rate significantly improves solution quality

Downloaded from https://www.cambridge.org/core. 17 Nov 2026 at 23:48:34, subject to the Cambridge Core terms of use.

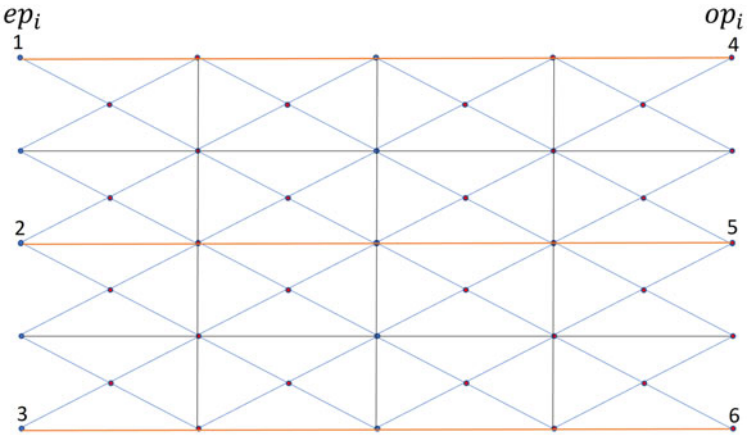


Figure 2. *A discretised airspace.*

compared to a lower rate within an acceptable solution time; however, further increasing the discretisation rate results in a significant increase in solution time without providing an equivalent improvement in solution quality. Therefore, the discretisation of the airspace into 41 points was chosen to provide sufficient routeing flexibility while maintaining a reasonable balance between computational efficiency and the solution quality of the trajectory optimisation.

Similarly, the number of entry and exit points was determined by balancing routeing flexibility and computational efficiency, consistent with the methodology of Reference [33]. Given that the study focuses on a single flight level within a 120 nm × 120 nm airspace, selecting a moderate number of entry and exit points (e.g. three entry and three exit points) ensures diverse traffic flows while maintaining a manageable model complexity.

In this study, potential conflict points are determined based on intersections of possible flight trajectories within a discretised free route airspace, particularly where multiple aircraft routes intersect given their entry and exit point combinations. These points are selected to approximate potential conflict points while preserving the flexibility of free route operations and to ensure that all feasible conflicts can be monitored without scanning the entire airspace. These points are critical for both conflict resolution and convective weather avoidance, facilitating the determination of flight routes between airspace entry and exit points. By utilising these points, the study explores efficient route planning and enhanced safety measures within the airspace, thereby optimising ATFM under various operational conditions.

3. Methodology

3.1. General methodology

Figure 3 shows the general methodology of this study. Initially, we developed a deterministic model based on the airspace discretisation technique. This model assumes that convective areas are static and predictable over a certain period, allowing for a structured approach to conflict detection and resolution. Given the short-term predictability of convective weather conditions, this provides a reliable basis for trajectory planning within each planning horizon. However, this assumption is limited to each 15-min planning horizon and does not imply static conditions over the entire operation. Subsequently, we developed a stochastic model to consider wind uncertainties, addressing the variability in wind conditions. To address the dynamic nature of convective weather over time, we applied the RHC approach to both the deterministic and stochastic models. RHC is a sequential decision-making process in which the planning horizon is periodically rolled forward (e.g. every 10 min), allowing the model to incorporate updated weather information and adjust aircraft trajectories accordingly. This comprehensive and adaptable control strategy effectively addresses both predictable elements and uncertainties in ATM.

Downloaded from https://www.cambridge.org/core. 17 Nov 2026 at 23:48:34, subject to the Cambridge Core terms of use.

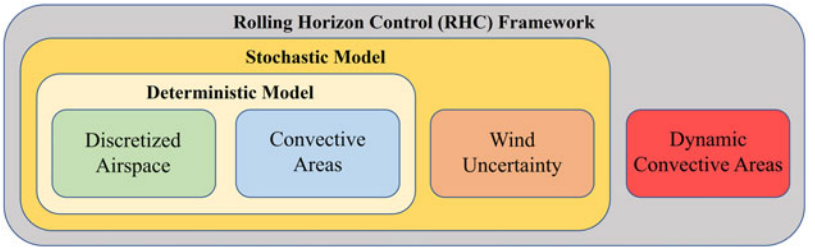


Figure 3. *General methodology of the study.*

3.2. Two-stage stochastic programming

Stochastic programming is an optimisation method that models problems with uncertain parameters assessed through historical data or expert opinions. It often employs recourse models, where the initial decision is made before uncertainties are fully known. Once uncertainties reveal themselves, adjustments are made to this decision, followed by further decisions. The two-stage stochastic model is a common approach where an initial decision precedes the realisation of uncertainties. In the second stage, a subsequent recourse decision is made in response to new information [55, 56].

The two-stage stochastic programming approach is used to account for uncertainties in wind conditions, which significantly affect flight planning and airspace management. This method allows for incorporating variable wind speeds and directions into the optimisation process, enhancing the robustness of the resulting flight trajectories [57].

The two-stage stochastic programming model can be mathematically formulated as given in Equations (s1–s4) [58]:

$$min\, c^T x + E\left[Q\left(x, \xi\right)\right] \tag{2s}$$

$$s.t.\, Ax = b, x \geq 0 \tag{3s}$$

where $Ax = b$ represents the set of constraints, x represents the vector of the first-stage decision variables along with the coefficient vector c^T. $E[Q(x, \xi)]$ denotes the expected cost of the second-stage decisions, given the first-stage decisions x and the random variable ξ representing uncertainties [58]. $Q(x, \xi)$ represents the solution of the second-stage problem as given:

$$min\, q\left(\xi\right)^T y \tag{4s}$$

$$s.t.\, T\left(\xi\right) x - W\left(\xi\right) y = h\left(\xi\right), y \geq 0 \tag{5s}$$

where y represents the second-stage decision variables. The second-stage problem is determined by the data $\xi = (q, h, T, W)$, where any or all of these elements can be random. T is referred to as the technology matrices, while W is referred to as recourse matrices. q and h are the second-stage objective vector and the right-hand side vector in the second stage, respectively Reference [58].

In the second stage, the model incorporates wind uncertainties into the optimisation process. Wind conditions are considered random variables with known probability distributions, reflecting atmospheric conditions' inherent variability and unpredictability. The objective is to adjust the initial deterministic trajectories to account for these uncertainties, thereby minimising the total expected flight time and potential conflicts under varying wind scenarios.

Uncertainty can be represented in two ways: continuous probability distributions or discrete event approach. The discrete event approach, also known as the scenario-based approach, is used instead of continuous probability distributions because it simplifies the computational complexity of the problem [59]. The scenario-based stochastic approach was introduced by Reference [60]. By discretising the possible results into a finite set of scenarios, we can more effectively model and solve the optimisation problem. This approach allows for a more manageable and practical representation of uncertainties, making it easier to incorporate into the optimisation process [61]. In this approach, the random vector ξ is

Downloaded from https://www.cambridge.org/core. 17 Nov 2026 at 23:48:34, subject to the Cambridge Core terms of use.

represented by a finite number of possible scenarios $\xi_1, \xi_2, \ldots, \xi_s$, each associated with a specific probability $p_1, p_2, \ldots, p_s$. Consequently, the expectation in the objective function of the first-stage problem is expressed as shown in Equation (s5) [62].

$$E\left[Q\left(x, \xi\right)\right] = \sum_{s=1}^{S} p_S Q\left(x, \xi_S\right) \tag{6s}$$

The value of the stochastic solution (VSS) is a measure used to quantify the benefit of using a stochastic model over a deterministic one [58]. In this study, VSS is used to assess the benefits of using a stochastic model to account for uncertainties in wind direction and speed in flight planning. To calculate VSS, we compare the expected performance of the stochastic solution with that of the deterministic solution. This involves the following steps [63]:

Step 1: Solve the stochastic programming problem considering all scenarios. The objective function value of the stochastic model (z_s) is calculated by considering the uncertainty scenarios and their probabilities.

Step 2: Solve the problem using the deterministic model based on the most likely scenario, which is determined by the highest probability among the random event scenarios. Flight routes are determined using this model. In this study, the deterministic model represents the problem more realistically by considering the highest probability wind scenario, as wind effects are more significant when convective areas occur.

Step 3: Fix the flight routes determined in the previous step and solve the stochastic programming model again. Calculate the expected value of the objective function for this solution (z_v).

Step 4: Calculate the difference between the z_v and z_s values to determine the VSS value, as given in Equation (s6):

$$VSS = z_v - z_s \tag{7s}$$

A positive VSS indicates that the stochastic solution provides a better expected result than the deterministic solution, demonstrating the necessity of implementing stochastic programming. A higher VSS indicates greater benefits from considering wind uncertainties, leading to more robust and efficient flight trajectories.

3.3. Determination of wind scenarios

Wind scenarios were generated for use in the stochastic programming model developed in this study. The process involved collecting, filtering and statistically analysing meteorological data collected during periods of convective areas to ensure a more accurate representation of the operational environment.

3.3.1. Data collection

For this study, the meteorological station in Kartal, Istanbul (station number 17064, 'Istanbul Region') was selected as the reference (Turkish State Meteorological [64]). Historical data from 2015 to 2023 was obtained using the 'meteomanz.com' and Iowa State University weather databases. Convective area periods were identified by detecting 'CB' (cumulonimbus) cloud codes and 'thunderstorm' descriptions from Meteomanz.com [65], and 'TS' codes from the Iowa State University database (Iowa State [66]).

The datasets were cross-checked to accurately determine the specific days and times when convective areas occurred. A total of 26 days with convective weather events were identified, corresponding to 36 separate convective events. Non-consecutive events occurring on the same day with at least 1-hour gap were considered separate events. Subsequently, wind data for the identified days was obtained from the Wyoming University database for the Istanbul Kartal station [67]. This dataset includes wind direction

Downloaded from https://www.cambridge.org/core. 17 Nov 2026 at 23:48:34, subject to the Cambridge Core terms of use.

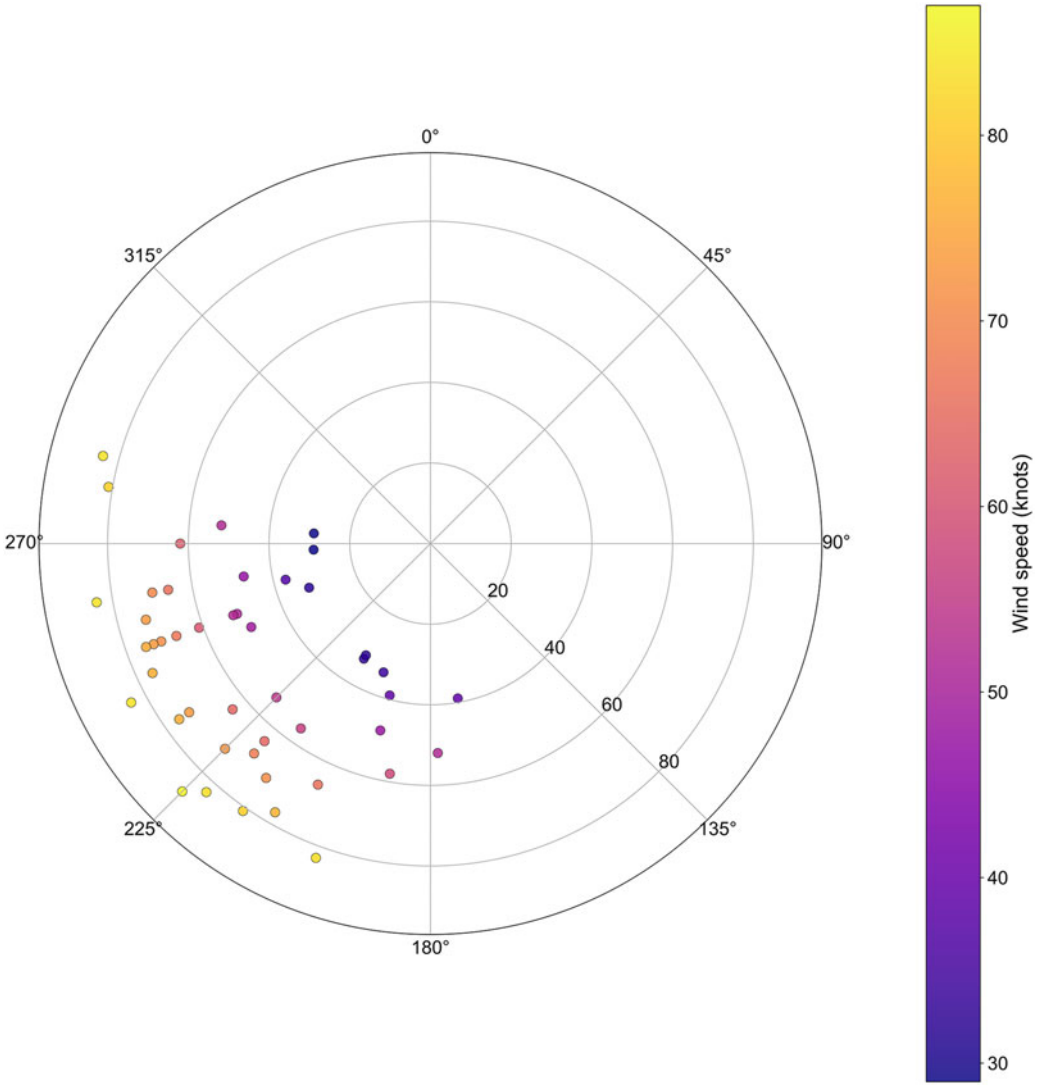


Figure 4. *Wind direction and speed distribution at FL350.*

(in degrees) and wind speed (in knots) at various altitudes. These data were filtered for FL350, resulting in 47 wind observations. The corresponding wind direction and speed distribution is shown in Figure 4.

A spatially uniform upper-air wind field was assumed within the modelled airspace. This assumption was adopted because direct upper-air wind observations at cruising altitude are limited, and the Kartal station is the only one providing upper-air measurements in the Istanbul region. The modelled airspace was selected such that the Kartal station is located as close as possible to its geometric centre, and the identified convective weather events occurred close to the station, thereby improving the representativeness of the available wind observations for the modelled airspace.

3.3.2. Data analysis

The collected wind data were analysed to identify their statistical characteristics. Following consultations with meteorological experts, the key variables, wind direction and wind speed, were categorised into specific ranges to support scenario generation.

Downloaded from https://www.cambridge.org/core. 17 Nov 2026 at 23:48:34, subject to the Cambridge Core terms of use.

Table 2. *Five wind scenarios and probabilities*

Scenarios	Direction	Speed	Probability (%)
s1	195	39	11.8
s2	195	59	17.6
s3	195	79	11.8
s4	255	59	26.5
s5	255	79	32.4

Wind directions were divided into six 60° intervals (45°–105°, 105°–165°, 165°–225°, 225°–285°, 285°–345° and 345°–45°). These intervals were shifted by half a sector (30°) from the 0° axis so that each sector represents a central wind direction. This half-sector shift ensures that typical wind directions are in the middle of their respective sectors, rather than on the boundaries, thereby avoiding ambiguity in boundary cases.

Wind speeds were classified into 20-knot intervals, starting from the minimum observed value of 29 knots and extending to the highest observed value of 87 knots. This produced three intervals that fully cover the observed speed range. Each observation was then assigned to its corresponding direction and speed interval class, and the frequency of occurrence within each combination was calculated. Based on these frequencies, five representative wind scenarios were derived to capture the wind conditions during convective activity. The probability of each scenario reflects its relative frequency in the dataset. These wind scenarios and their associated probabilities are presented in Table 2.

To quantitatively assess how well the representative scenarios approximate the original observations, each observation retained for the representative-scenario analysis was compared with its corresponding representative scenario. The mean and maximum absolute wind-speed approximation errors were calculated, together with the mean and maximum circular wind-direction errors. The mean wind-speed approximation error was 5.32 knots, with a maximum error of 10 knots, while the mean circular wind-direction error was 14.07°, with a maximum error of 30°. These results provide a quantitative assessment of the degree to which the five representative scenarios reproduce the observed wind conditions.

3.4. Impact on flight speeds

Aircraft GS should be used instead of TAS because flight speeds are influenced by wind speed and direction. GS accounts for the effects of wind, providing a more accurate measure of the actual speed of aircraft over the ground. GS can be calculated using Equation (s7).

$$V_{ground} = V_{TAS} + V_{wind} \cos\left(AC_{track} - Wind_{direction}\right) \tag{8s}$$

where V_{wind} represents the wind speed, $Wind_{direction}$ represents the wind direction and represents AC_{track} the aircraft's track. The track of each aircraft is equal to the direction of the flight path between pairs of points along the trajectory.

3.5. RHC approach

The RHC approach, originally introduced in the early 1960s by References [68] and [69] for linear systems using linear programming, has been adapted in this study to optimise aircraft trajectories under dynamic convective weather conditions. The RHC approach optimises dynamic problems by solving a sequence of sub-problems over a rolling time horizon where only the first segment of the solution is implemented before the model is updated and reoptimised for the next decision step. This iterative process improves adaptability and responsiveness to real-time changes in operational constraints and environmental conditions [70]. At each decision point, the model optimises flight trajectories for a future

Downloaded from https://www.cambridge.org/core. 17 Nov 2026 at 23:48:34, subject to the Cambridge Core terms of use.

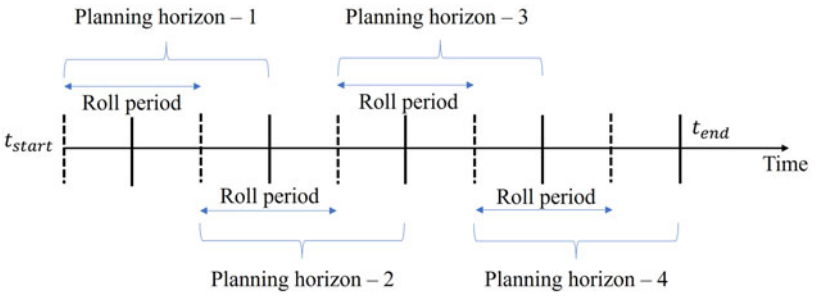


Figure 5. *RHC approach.*

period known as the planning horizon. Once the optimal solution for this period is determined, only the initial segment, referred to as the roll period, is implemented, and the horizon rolls forward, repeating the process with updated data [71, 72].

In this approach, the problem is divided into planning horizons that can be solved individually or in an overlapping manner. Independent solving generates solutions without sharing information between the horizons, while overlapping solving allows information flow between them. In other words, a portion of the trajectory gets reoptimised multiple times as the horizon slides forward, allowing earlier decisions to be improved with updated information. The overlapping RHC approach used in this study is shown in Figure 5 for a specific start (t_{start}) and end time (t_{end}). This approach increases computational complexity but results in higher quality solutions due to better information sharing [73–75].

3.6. Determination of convective areas

The dates and times of convective weather for the meteorological station in Kartal, Istanbul, were identified using data from the Iowa State University database and the Meteomanz.com website (Iowa State [65, 66]. Weather radar images corresponding to these dates and times were then obtained from the Turkish State Meteorological [64]. The radar images provide information on the observation time, date, maximum range and radar reflectivity (dBZ). A reflectivity threshold of 21 dBZ or greater was used to identify convective areas within the 120 × 120 NM modelled airspace. As illustrated in Figure 6, the purple dashed frame represents the modelled airspace, while the red outlines indicate the boundaries of the identified convective areas. These boundaries were manually digitised from the radar images and subsequently spatially transferred and overlaid onto the corresponding airspace representation used in the trajectory optimisation model, as shown in Figure 7.

In order to evaluate the performance of the proposed models under different weather dynamics, five different convective area cases (CB-1, CB-2, CB-3, CB-4, CB-5) were defined based on radar data obtained from the Turkish State Meteorological Service. These cases represent different spatial and temporal evolution of convective areas. For example, while CB-1 reflects expanding and merging convective areas over time, CB-5 features areas that shrink and dissipate. This categorisation makes it possible to evaluate the adaptability of models to different operational cases. Figure 7 provides an overview of a representative convective area. Detailed airspace configurations and descriptions of all five cases are provided in the cases and test problems section and in Appendix A.

4. Mathematical model

This section presents the mathematical models developed to optimise trajectories of aircraft set $A = (1, 2, \ldots, a)$ within the specified airspace under convective weather conditions and wind uncertainties. Using the airspace discretisation technique, the airspace is defined by a set of flight points $F = (1, 2, \ldots, f)$. Aircraft enter the airspace at points belonging to the set $E = (1, 2, \ldots, e)$ and exit at points belonging to the set $O = (1, 2, \ldots, o)$.

Downloaded from https://www.cambridge.org/core. 17 Nov 2026 at 23:48:34, subject to the Cambridge Core terms of use.

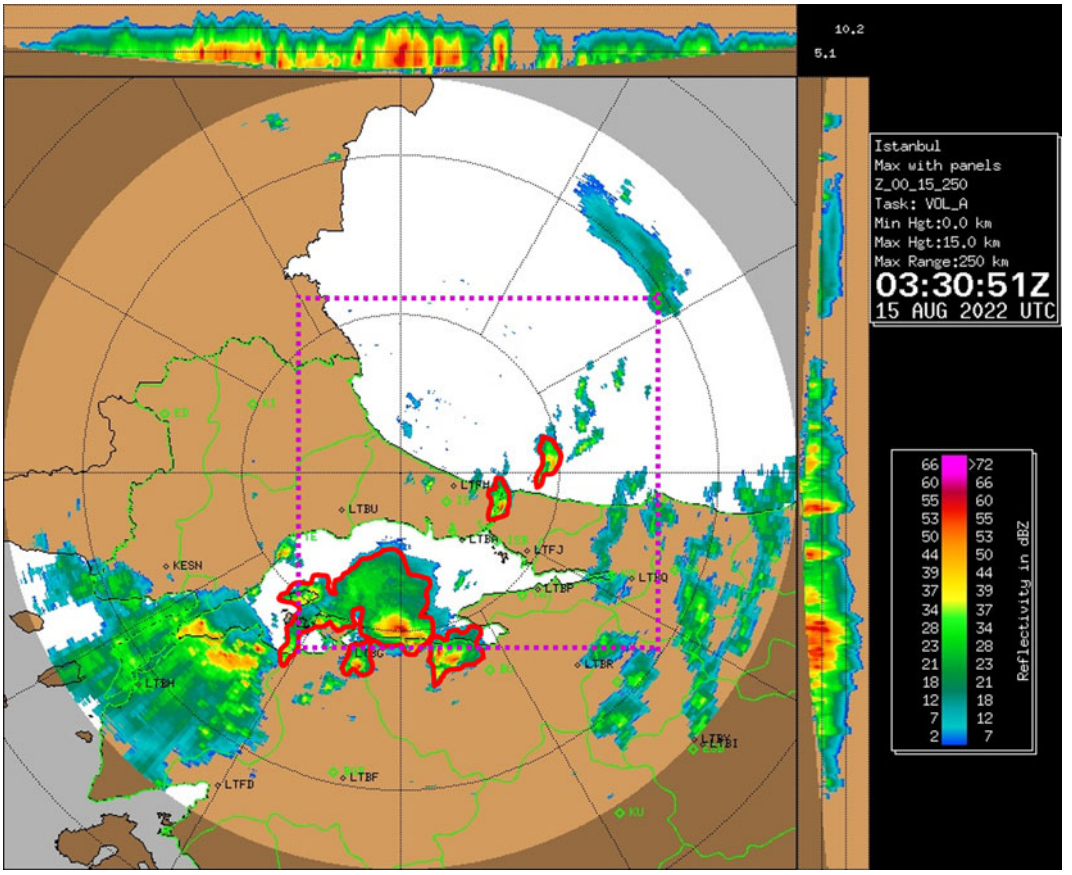


Figure 6. *Istanbul weather radar image and identified convective areas.*

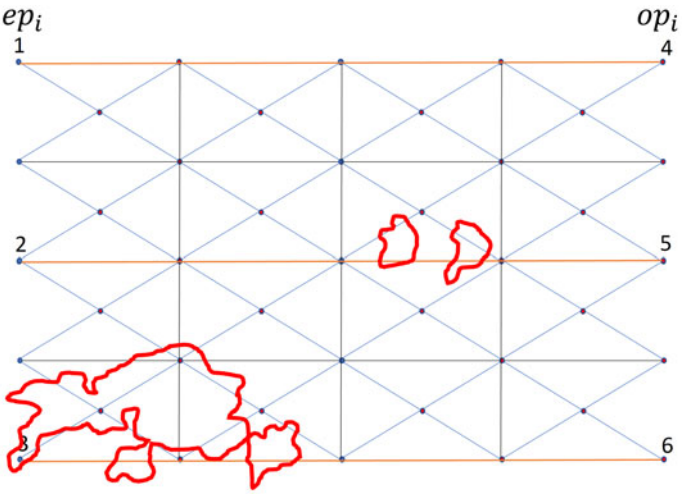


Figure 7. *Spatial representation of identified convective areas in the modelled airspace.*

Downloaded from https://www.cambridge.org/core. 17 Nov 2026 at 23:48:34, subject to the Cambridge Core terms of use.

4.1. Deterministic model

Indices

$i, j \in A$	Aircraft indices
$m, n, k \in F$	Flight point indices

Parameters

ep_i	The airspace entry point of aircraft i
op_i	The airspace exit point of aircraft i
et_i	Estimated airspace entry time of aircraft i
$b_{m,n}$	Binary parameter indicating whether the flight between points m and n is possible under convective weather conditions (1 if possible, 0 otherwise)
$d_{m,n}$	Distance matrix for routes between points m and n
v_i	TAS of aircraft i
$sep^{mrg}_{v_i,v_j m,k,n}$	Separation time at point n between aircraft i flying from point m and aircraft j flying from point k, with TAS v_i and v_j
$sep^{div}_{v_i,v_j m,n,k}$	Separation time at point n between aircraft i flying from point m and aircraft j flying to point k, with TAS v_i and v_j
$sep^{head}_{v_i,v_j m,n,m}$	Head-on separation time between aircraft j flying from m to n and aircraft i entering the n to m segment, ensuring that aircraft i reaches point n at least sep^{head} after aircraft j passes point n
G	Big enough positive number

Decision variables

$t_{i,m}$	The time at which aircraft i passes point m
$x_{i,m,n}$	The binary variable equals 1 if aircraft i flies from point m to point n; otherwise, it is 0
$r_{i,j,n}$	The binary variable equals 1 if aircraft i reaches point n before aircraft j; otherwise, it is 0

Objective function

After entering the airspace, pilots aim to reach the exit points in the shortest possible time. The objective of this study is to minimise the total flight time for all aircraft within the defined airspace. This objective is mathematically represented in Equation (2).

$$z_{det} = min \sum_{i \in A} \sum_{m \in F} \sum_{n \in F} \frac{x_{i,m,n} d_{m,n}}{v_i} \tag{2}$$

Constraints

Assignment constraints

The assignment constraints in Equations (3)–(6) ensure that each aircraft follows a valid trajectory through the airspace, entering and exiting at the predefined points while avoiding convective areas. Equation (3) determines the initial route that each aircraft i takes from its entry point ep_i once it enters the airspace. Subsequently, Equation (4) assigns all the routes that each aircraft will fly within the airspace until it reaches the exit point. Since the next point an aircraft arrives after the entry point is determined by the previous constraint, the entry point is excluded from the conditions of this equation. Additionally, Equation (5) assigns the last point that each aircraft i arrives before leaving the airspace at point op_i, hence the exit point is excluded from Equation (4). When assigning flight routes in Equations (3)–(5), it is ensured that there is a connection between points m and n (i.e. $d_{m,n} \neq 0$) and that the route is not closed due to convective weather conditions ($b_{m,n} = 1$). Equation (6) ensures that no assignments are made if either of these conditions is not met.

$$\sum_{\substack{m \in F \\ m \neq n \\ m = ep_i}} \sum_{\substack{n \in F \\ d_{m,n} \neq 0 \\ b_{m,n} = 1}} x_{i,m,n} = 1 \qquad \forall i \tag{3}$$

Downloaded from https://www.cambridge.org/core. 17 Nov 2026 at 23:48:34, subject to the Cambridge Core terms of use.

$$\sum_{\substack{n \in F \\ n \neq m \\ n \neq ep_i \\ d_{m,n} \neq 0 \\ b_{m,n} = 1}} x_{i,m,n} - \sum_{\substack{n \in F \\ n \neq m \\ n \neq op_i \\ d_{m,n} \neq 0 \\ b_{n,m} = 1}} x_{i,n,m} = 0 \qquad \forall i, m \quad m \neq ep_i, m \neq op_i \tag{4}$$

$$\sum_{\substack{m \in F \\ m \neq n \\ b_{m,n} = 1}} \sum_{\substack{n \in F \\ n = op_i \\ d_{m,n} \neq 0}} x_{i,m,n} = 1 \qquad \forall i \tag{5}$$

$$\sum_{m \in F} \sum_{\substack{n \in F \\ d_{m,n} = 0 \\ or \\ b_{m,n} = 0}} x_{i,m,n} = 0 \qquad \forall i \tag{6}$$

Time calculation constraints

Constraints (7) and (8) determine the time at which each aircraft i will be at the point immediately after its entry point ep_i. The times at which the aircraft will be present at all points along the formed trajectory are calculated using Constraints (9) and (10). Since the time at the next point after the entry point is ensured by the first two equations, the entry point is excluded from the conditions of these equations.

$$t_{i,n} \geq et_i + \frac{d_{m,n}}{v_i} - G(1 - x_{i,m,n}) \qquad \forall i, n, m = ep_i \tag{7}$$

$$t_{i,n} \leq et_i + \frac{d_{m,n}}{v_i} + G(1 - x_{i,m,n}) \qquad \forall i, n, m = ep_i \tag{8}$$

$$t_{i,n} \geq t_{i,m} + \frac{d_{m,n}}{v_i} - G(1 - x_{i,m,n}) \qquad \forall i, m, n \quad m \neq n, m \neq ep_i \tag{9}$$

$$t_{i,n} \leq t_{i,m} + \frac{d_{m,n}}{v_i} + G(1 - x_{i,m,n}) \qquad \forall i, m, n \quad m \neq n, m \neq ep_i \tag{10}$$

Separation constraints

In the airspace, aircraft operations must be conducted along conflict-free trajectories. To ensure safe separation, the mathematical model incorporates separation constraints to prevent conflicts at intersection points and route segments. Specifically, Constraints (11) and (12) define the merging conditions to ensure that aircraft approaching a common waypoint from different incoming routes maintain the required minimum separation. Furthermore, Constraints (13) and (14) define the separation required when a leading aircraft diverges onto a subsequent route segment while a trailing aircraft approaches the same intersection point. To manage head on conflicts, Constraints (15) and (16) ensure that the aircraft entering the segment first clears the exit node before the opposing aircraft arrives at the same point, maintaining at least the specified time separation between the two aircraft. Finally, Constraints (17) and (18) define the no-overtaking conditions to preserve the sequence of aircraft along the route segments and prevent conflicts arising from differences in the speeds of leading and trailing aircraft.

$$t_{i,n} \geq t_{j,n} + sep^{mrg}_{v_i,v_j m,k,n} - G(2 - x_{i,m,n} - x_{j,k,n}) - Gr_{i,j,n} \qquad \forall i, j, m, k, n \quad i \neq j, m \neq n, k \neq n, n \neq ep_i \quad d_{m,n} \neq 0, d_{k,n} \neq 0 \tag{11}$$

Downloaded from https://www.cambridge.org/core. 17 Nov 2026 at 23:48:34, subject to the Cambridge Core terms of use.

$$t_{j,n} \geq t_{i,n} + sep^{mrg}_{v_j,v_i m,k,n} - G(2 - x_{j,m,n} - x_{i,k,n}) - G(1 - r_{i,j,n}) \qquad \forall i,j,m,k,n \quad i \neq j, m \neq n, k \neq n, n \neq ep_i \quad d_{m,n} \neq 0, d_{k,n} \neq 0 \tag{12}$$

$$t_{i,n} \geq t_{j,n} + sep^{div}_{v_i,v_j m,n,k} - G(2 - x_{i,m,n} - x_{j,n,k}) - Gr_{i,j,n} \qquad \forall i,j,m,k,n \quad i \neq j, m \neq n, n \neq k, m \neq k \quad n \neq ep_i, n \neq op_i \quad d_{m,n} \neq 0, d_{n,k} \neq 0 \tag{13}$$

$$t_{j,n} \geq t_{i,n} + sep^{div}_{v_j,v_i m,n,k} - G(2 - x_{j,m,n} - x_{i,n,k}) - G(1 - r_{i,j,n}) \qquad \forall i,j,m,k,n \quad i \neq j, m \neq n, n \neq k, m \neq k \quad n \neq ep_i, n \neq op_i \quad d_{m,n} \neq 0, d_{n,k} \neq 0 \tag{14}$$

$$t_{i,m} \geq t_{j,m} + sep^{head}_{v_i,v_j m,n,m} - G(2 - x_{i,m,n} - x_{j,n,m}) - Gr_{i,j,n} \qquad \forall i,j,m,n \quad i \neq j, m \neq n, m \neq ep_i, n \neq ep_i \quad d_{m,n} \neq 0, d_{n,m} \neq 0 \tag{15}$$

$$t_{j,n} \geq t_{i,n} + sep^{head}_{v_j,v_i n,m,n} - G(2 - x_{i,m,n} - x_{j,n,m}) - G(1 - r_{i,j,n}) \qquad \forall i,j,m,n \quad i \neq j, m \neq n, m \neq ep_i, n \neq ep_i \quad d_{m,n} \neq 0, d_{n,m} \neq 0 \tag{16}$$

$$t_{i,n} - \frac{d_{m,n}}{v_i} \geq t_{j,n} - \frac{d_{m,n}}{v_j} - G(2 - x_{i,m,n} - x_{j,m,n}) - Gr_{i,j,n} \qquad \forall i,j,m,n \quad i \neq j, d_{m,n} \neq 0 \tag{17}$$

$$t_{j,n} - \frac{d_{m,n}}{v_j} \geq t_{i,n} - \frac{d_{m,n}}{v_i} - G(2 - x_{i,m,n} - x_{j,m,n}) - G(1 - r_{i,j,n}) \qquad \forall i,j,m,n \quad i \neq j, d_{m,n} \neq 0 \tag{18}$$

4.2. Stochastic model

The stochastic model of the problem is presented below, along with the additional indices, parameters and decision variables that are specific to this formulation and differ from those defined in the deterministic model.

Indices

$s \in S$	Wind scenarios indices

Parameters

$v_{i,m,n,s}$	GS of the aircraft i between points m and n in the wind scenario s
$prob_s$	Probability of each wind scenario s
$sep^{mrg}_{v_i,v_j m,k,n,s}$	Separation time at point n between aircraft i flying from point m and aircraft j flying from point k, with GS v_i and v_j under wind scenario s
$sep^{div}_{v_i,v_j m,n,k,s}$	Separation time at point n between aircraft i flying from point m and aircraft j flying to point k, with GS v_i and v_j under wind scenario s
$sep^{head}_{v_i,v_j m,n,m,s}$	Head on separation time between aircraft j flying from m to n and aircraft i entering the n to m segment, with GS v_i and v_j under wind scenario s

Downloaded from https://www.cambridge.org/core. 17 Nov 2026 at 23:48:34, subject to the Cambridge Core terms of use.

First stage decision variables

$x_{i,m,n}$ The binary variable equals 1 if aircraft i flies from point m to point n; otherwise, it is 0

Second stage decision variables

$t_{i,m,s}$ The time at which aircraft i passes point m in wind scenario s

$r_{i,j,n,s}$ The binary variable that equals 1 if aircraft i reaches point n before aircraft j in wind scenario s; otherwise, it is 0

$total_time_s$ Total flight time of aircraft in wind scenario s

Objective function

Equation (19) calculates the total flight time of each scenario. The objective function of the stochastic model aims to minimise the expected total flight time for all scenarios, considering uncertainties in wind conditions as given in Equation (20).

$$total_time_s = \sum_{i \in A} \sum_{m \in F} \sum_{n \in F} \frac{x_{i,m,n} d_{m,n}}{v_{i,m,n,s}} \quad \forall s \tag{19}$$

$$z_{sto} = min \sum_{s} prob_s total_time_s \tag{20}$$

Assignment constraints

In the stochastic model, the trajectory assignment constraints that determine the trajectories of the aircraft are the same as those in the deterministic model (Equations (3)–(6)). All the decision variables involved in the assignment constraints are first stage decision variables in the stochastic model. Therefore, the assignment constraints do not include the s indices representing wind scenarios.

Time calculation constraints

After entering the airspace, the times at which aircraft will be present at each point along their trajectories are calculated using Constraints (21)–(24). The speeds of the aircraft are dependent on the wind direction and wind speed within the airspace. Therefore, the GS of the aircraft, as given by Equation (s7), must be considered. The times at which aircraft will be present at each point along the determined flight trajectories are calculated by considering the flight track, wind direction and wind speed. This ensures that the model determines the trajectories of the flights by considering all wind uncertainty scenarios.

$$t_{i,n,s} \geq et_i + \frac{d_{m,n}}{v_{i,m,n,s}} - G(1 - x_{i,m,n}) \qquad \forall i, m, n, s \quad m = ep_i \tag{21}$$

$$t_{i,n,s} \leq et_i + \frac{d_{m,n}}{v_{i,m,n,s}} + G(1 - x_{i,m,n}) \qquad \forall i, m, n, s \quad m = ep_i \tag{22}$$

$$t_{i,n,s} \geq t_{i,m,s} + \frac{d_{m,n}}{v_{i,m,n,s}} - G(1 - x_{i,m,n}) \qquad \forall i, m, n, s \quad m \neq n, m \neq ep_i \tag{23}$$

$$t_{i,n,s} \leq t_{i,m,s} + \frac{d_{m,n}}{v_{i,m,n,s}} + G(1 - x_{i,m,n}) \qquad \forall i, m, n, s \quad m \neq n, m \neq ep_i \tag{24}$$

Separation constraints

In the stochastic formulation of the model, the separation conditions are adapted to represent wind uncertainty through the scenario index s. Constraints (25)–(32) serve the same purpose as their deterministic counterparts, ensuring conflict-free merging, diverging, trailing and head-on operations. In the stochastic formulation, however, the separation time parameters vary across scenarios according to the prevailing wind conditions. Specifically, GS of the aircraft on each flight segment, which vary according

Downloaded from https://www.cambridge.org/core. 17 Nov 2026 at 23:48:34, subject to the Cambridge Core terms of use.

to the scenario, are considered when calculating the stochastic separation times.

$$t_{i,n,s} \geq t_{j,n,s} + sep^{mrg}_{v_i,v_j m,k,n,s} - G(2 - x_{i,m,n} - x_{j,k,n}) - Gr_{i,j,n,s} \qquad \forall i,j,m,k,n,s \quad i \neq j, m \neq n, k \neq n, n \neq ep_i \quad d_{m,n} \neq 0, d_{k,n} \neq 0 \tag{25}$$

$$t_{j,n,s} \geq t_{i,n,s} + sep^{mrg}_{v_j,v_i m,k,n,s} - G(2 - x_{j,m,n} - x_{i,k,n}) - G(1 - r_{i,j,n,s}) \qquad \forall i,j,m,k,n,s \quad i \neq j, m \neq n, k \neq n, n \neq ep_i \quad d_{m,n} \neq 0, d_{k,n} \neq 0 \tag{26}$$

$$t_{i,n,s} \geq t_{j,n,s} + sep^{div}_{v_i,v_j m,n,k,s} - G(2 - x_{i,m,n} - x_{j,n,k}) - Gr_{i,j,n,s} \qquad \forall i,j,m,k,n,s \quad i \neq j, m \neq n, n \neq k, m \neq k \quad n \neq ep_i, n \neq op_i \quad d_{m,n} \neq 0, d_{n,k} \neq 0 \tag{27}$$

$$t_{j,n,s} \geq t_{i,n,s} + sep^{div}_{v_j,v_i m,n,k,s} - G(2 - x_{j,m,n} - x_{i,n,k}) - G(1 - r_{i,j,n,s}) \qquad \forall i,j,m,k,n,s \quad i \neq j, m \neq n, n \neq k, m \neq k \quad n \neq ep_i, n \neq op_i \quad d_{m,n} \neq 0, d_{n,k} \neq 0 \tag{28}$$

$$t_{i,m,s} \geq t_{j,m,s} + sep^{head}_{v_i,v_j m,n,m,s} - G(2 - x_{i,m,n} - x_{j,n,m}) - Gr_{i,j,n,s} \qquad \forall i,j,m,n,s \quad i \neq j, m \neq n, m \neq ep_i \quad n \neq ep_i, d_{m,n} \neq 0, d_{n,m} \neq 0 \tag{29}$$

$$t_{j,n,s} \geq t_{i,n,s} + sep^{head}_{v_j,v_i n,m,n,s} - G(2 - x_{i,m,n} - x_{j,n,m}) - G(1 - r_{i,j,n,s}) \qquad \forall i,j,m,n,s \quad i \neq j, m \neq n, m \neq ep_i \quad n \neq ep_i, d_{m,n} \neq 0, d_{n,m} \neq 0 \tag{30}$$

$$t_{i,n,s} - \frac{d_{m,n}}{v_{i,m,n,s}} \geq t_{j,n,s} - \frac{d_{m,n}}{v_{j,m,n,s}} - G(2 - x_{i,m,n} - x_{j,m,n}) - Gr_{i,j,n,s} \qquad \forall i,j,m,n,s \quad i \neq j, d_{m,n} \neq 0 \tag{31}$$

$$t_{j,n,s} - \frac{d_{m,n}}{v_{j,m,n,s}} \geq t_{i,n,s} - \frac{d_{m,n}}{v_{i,m,n,s}} - G(2 - x_{i,m,n} - x_{j,m,n}) - G(1 - r_{i,j,n,s}) \qquad \forall i,j,m,n,s \quad i \neq j, d_{m,n} \neq 0 \tag{32}$$

5. Implementation of the RHC

The parameters used to establish the timeline for the RHC approach are defined as follows:

t_{start}	RHC start time
t_{end}	RHC end time
t_{period}	Roll period length
$t_{horizon_period}$	Start time of each planning horizon
$t_{horizon_start}$	Planning horizon period length
$t_{horizon_end}$	End time of each planning horizon
t_{win}	Roll period end time for each planning horizon

Downloaded from https://www.cambridge.org/core. 17 Nov 2026 at 23:48:34, subject to the Cambridge Core terms of use.

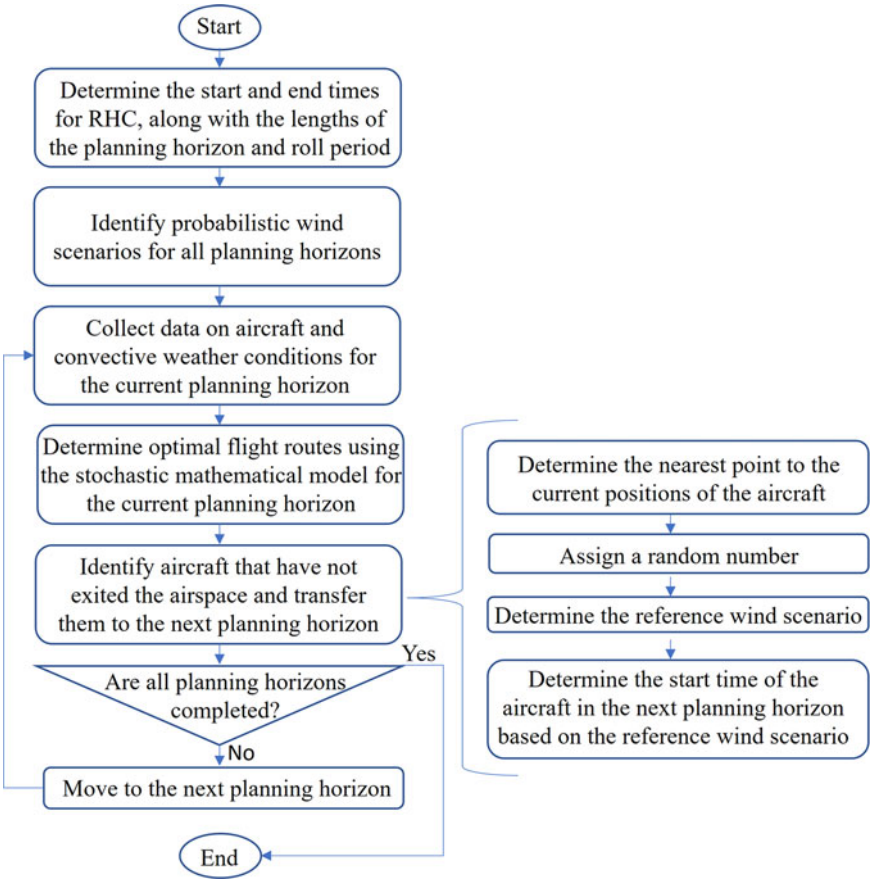


Figure 8. *RHC flowchart.*

The roll period end time for each planning horizon corresponds to the time given in Equation (33). The planning horizon period length is the same for all periods. The end times of all planning horizons are calculated using Equation (34):

$$t_{win} = t_{horizon_start} + t_{period} \tag{33}$$

$$t_{horizon_end} = t_{horizon_start} + t_{horizon_period} \tag{34}$$

To effectively manage the dynamic behaviour of convective areas, updating them at intervals matching the planning horizon period is essential. The literature typically uses 15-min update intervals [45, 51, 52, 76–78], reflecting the regular update intervals of radar data [38, 79, 80]. Similarly, a typical value of the update interval for conflict resolution in two-dimensional trajectory planning is 10–15 min [20]. Therefore, this study adopts a 15-min planning horizon period ($t_{horizon_period} = 15\text{min}$) and a 10-min roll period length ($t_{period} = 10\text{min}$), consistent with common practice.

The flowchart of applying the RHC approach using the stochastic model, which includes convective areas and wind uncertainties under convective weather conditions, is shown in Figure 8. Based on the entry times of the aircraft into the airspace, it is determined whether they will be included in the current period. Aircraft with entry times within the interval $t_{horizon_start} - t_{horizon_end}$ are included in the current planning horizon. The model is solved after defining the necessary parameters for all aircraft in the current period. At the end of the roll period (t_{win}), aircraft that have not exited the airspace are identified

Downloaded from https://www.cambridge.org/core. 17 Nov 2026 at 23:48:34, subject to the Cambridge Core terms of use.

for inclusion in the next planning horizon. Their positions at t_{win} are determined, and the closest point to their current position is selected for the next period. To determine the start time at this point for the next planning horizon, a reference wind scenario is selected using a roulette wheel method based on the probabilities of the scenarios. It should be acknowledged that using a reference scenario to advance the time rather than propagating the entire distribution of possible start times is a modelling approximation. This prevents the exponential growth of the scenario tree and keeps the optimisation problem computationally tractable for operational applications. The starting points and times are then added to the relevant sets for the next period, where all wind scenarios are considered within the stochastic optimisation model. This process repeats for all planning horizons within the interval $t_{start} - t_{end}$.

6. Results

The mathematical models developed to ensure the safe operation of aircraft under convective weather conditions by avoiding convective areas and resolving conflicts between aircraft have been tested. All models were implemented in Python, and the optimisation problems were solved using the Gurobi Optimizer. The computations were performed on a 64-bit computer equipped with an Intel Core i9-14900HX processor (24 cores, 32 threads, up to 5.8 GHz) and 64 GB DDR5 RAM. This section discusses the test problems and results.

6.1. Cases and test problems

Convective areas obtained from the Turkish State Meteorological Service were analysed, and five different convective area cases (CB-1, CB-2, CB-3, CB-4, CB-5) were defined as described in the section on determination of convective areas. A total of 25 different test problems (TP-1, TP-2, . . ., TP-25) were produced, with 5 test problems for each convective area case. The wind scenarios listed in Table 2 are applied to all convective area cases and test problems. Each test problem consists of multiple planning horizons. The test problems in CB-1 and CB-2 cover a 50-min traffic period with five planning horizons and include 30 aircraft. CB-3, CB-4 and CB-5 cover a 60-min traffic period with six planning horizons, including 36 aircraft.

The parameters for the test problems include aircraft categories, estimated entry times into the airspace, entry points, and exit points. The distribution of aircraft categories is set at 50% medium and 50% heavy, with nominal TAS at FL350 set to 450 and 473 knots, respectively. Estimated entry times into the airspace are generated based on an exponential distribution, while entry and exit points are assigned randomly with equal probability.

The CB-5 case is selected as a representative example to illustrate the results obtained from the deterministic and stochastic models. The airspace views for the CB-5 case are shown in Figure 9. This case features convective areas that shrink and dissipate over time. The figure includes multiple sub-figures (a, b, c, d, e, f) that sequentially represent the time progression within the airspace. This allows for tracking the changes in convective areas over time, illustrating how these areas influence flight paths and airspace availability. Initially, aircraft aiming to travel from entry point 1 to exit point 5 have to navigate around the southern part of the airspace. However, from Figure 9(d), the opening of flight routes in the northeast enables shorter flight routes, as the shrinking and dissipation of convective areas increases the available airspace.

Detailed airspace views for the other four convective area cases (CB-1, CB-2, CB-3, CB-4) are provided in the Appendix A. CB-1 features a case where the convective areas grow and merge over time, significantly reducing the available airspace. Initially, aircraft enter from points 1 and 2, but navigating through the airspace becomes increasingly challenging as the convective areas expand. By the final planning horizon, exit point 4 is closed to flights due to the extensive coverage of convective areas. CB-2 presents a case with dynamic convective areas that grow and move, with some areas dissipating over time. This allows for changing flight paths, initially requiring longer routes but eventually opening shorter paths as convective areas shrink or dissipate. The northward movement of convective areas also

Downloaded from https://www.cambridge.org/core. 17 Nov 2026 at 23:48:34, subject to the Cambridge Core terms of use.

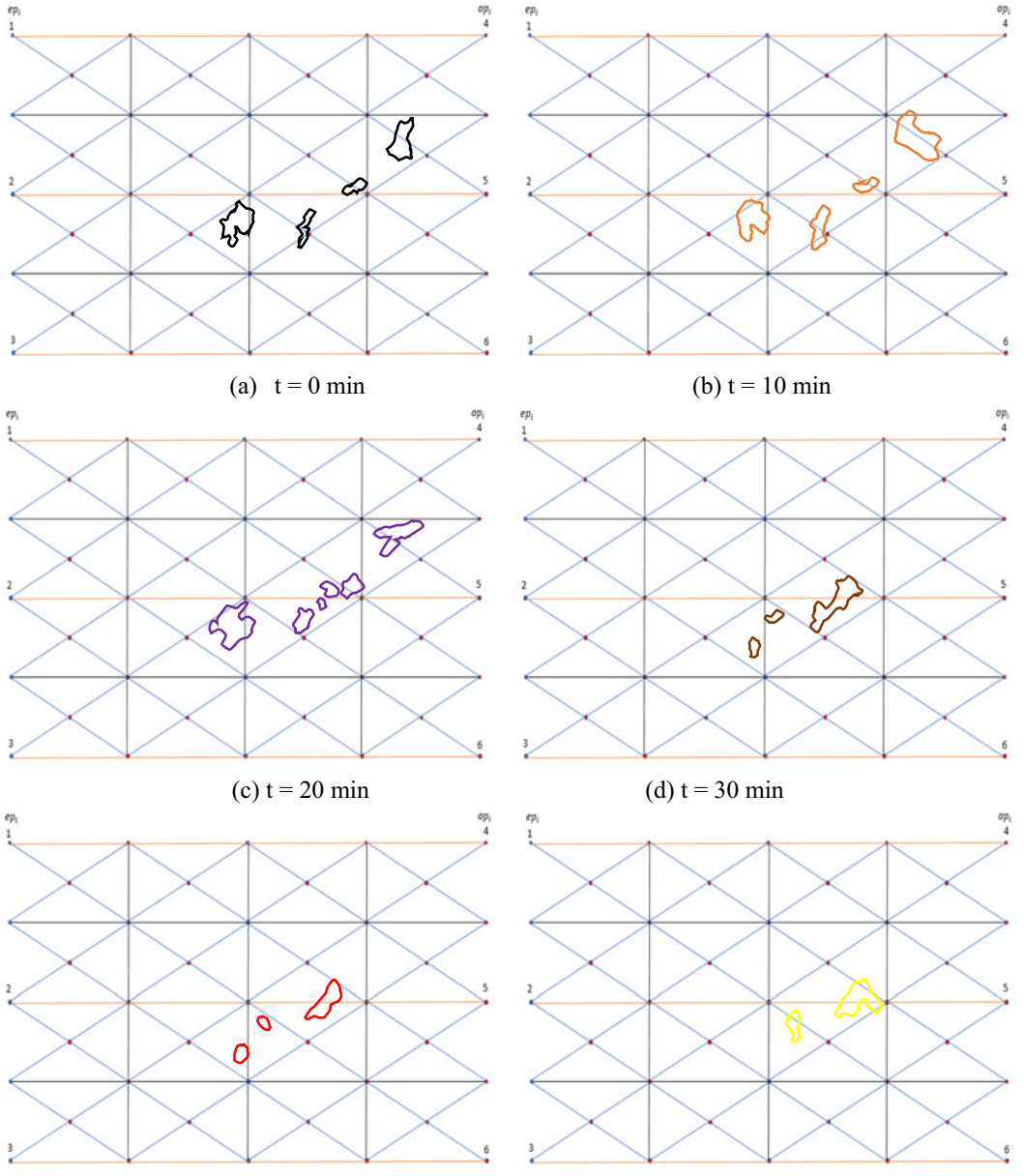


Figure 9. *The airspace views for the CB-5 case.*

impacts the available flight routes, particularly for aircraft entering from point 1. CB-3 displays a case where convective areas initially start small but grow over time. The convective areas remain nearly the same size but move eastward.

Additionally, new areas begin to form nearby and expand, covering a larger portion of the airspace. As the convective areas grow, the available airspace becomes more limited. CB-4 involves convective areas that shrink and dissipate over time. Initially, it is not possible for aircraft to operate from entry point 2. Therefore, aircraft enter the airspace from points 1 and 3 in the first two planning horizons. It is possible to enter from all three points starting from the third planning horizon. However, aircraft

Downloaded from https://www.cambridge.org/core. 17 Nov 2026 at 23:48:34, subject to the Cambridge Core terms of use.

Table 3. *Results of test problems in the CB-5 case*

Test problem	Planning horizon	Number of aircraft	z_s	Solution time	z_v	VSS
TP-21	1	12	15284	22	15627	343
	2	18	19768	291	- ∗	- ∗∗
	3	19	20269	216	20753	484
	4	20	17808	77	18221	413
	5	15	13341	29	13760	419
	6	13	10386	21	10715	329
TP-22	1	6	9143	8	9143	0
	2	12	16286	63	16484	198
	3	16	18366	245	- ∗	- ∗∗
	4	19	18380	48	18752	372
	5	20	16491	40	17012	521
	6	19	17146	81	17689	543
TP-23	1	9	13772	34	14156	384
	2	15	20939	379	- ∗	- ∗∗
	3	15	16765	120	17180	415
	4	20	19400	134	19699	300
	5	20	19507	222	19958	451
	6	19	17854	287	18414	560
TP-24	1	12	16125	23	16417	293
	2	19	20235	324	- ∗	- ∗∗
	3	19	20043	101	20520	476
	4	20	18247	150	18419	171
	5	16	13587	26	14014	427
	6	13	10210	16	10210	0
TP-25	1	6	9221	2	9221	0
	2	10	11726	6	12020	294
	3	16	17895	21	18455	560
	4	20	21866	329	- ∗	- ∗∗
	5	19	17638	204	18086	449
	6	22	18445	301	18875	430

∗ There is no feasible solution for the problem.
∗∗ VSS could not be calculated as the z_v objective function could not be obtained.

entering from point 2 and aiming for exit points 5 and 6 need to divert northwards, extending their flight paths. This case leads to a concentration of aircraft in the northern part of the airspace as they avoid convective areas.

6.2. Results of test problems in CB cases

The results of the test problems generated for the CB-5 case are presented in Table 3. The results of the other convective area cases are provided in Appendix B. The tables show the number of aircraft in each planning horizon, the objective function value of the stochastic model (z_s), the solution time for each stochastic model run, the objective function value obtained by fixing the trajectories obtained from the deterministic model and evaluating them under the stochastic model (z_v) and the VSS value, which represents the difference between the objective function values. The objective function values (z_s, z_v), VSS and computational solution times are reported in seconds.

Each test problem is evaluated over a sequence of consecutive planning horizons, with the number of aircraft varying across horizons. While the first planning horizon includes only the aircraft initially present in the airspace, subsequent horizons may include both aircraft newly entering the airspace and

Downloaded from https://www.cambridge.org/core. 17 Nov 2026 at 23:48:34, subject to the Cambridge Core terms of use.

aircraft transferred from previous horizons. At each planning horizon, the optimisation model determines trajectories for the aircraft present within the corresponding time interval, subject to the specified operational and separation constraints. Since aircraft entry and exit points are randomly generated, the resulting flight durations vary across aircraft. In addition, wind conditions significantly affect the flight time along the selected trajectories and are therefore considered in the optimisation process to obtain efficient flight trajectories.

The test problems exhibit substantial differences in total flight time across planning horizons, even when the number of aircraft is the same. Conversely, a planning horizon with more aircraft may result in a shorter total flight time than a horizon with fewer aircraft. These variations can be attributed to several factors, including the randomly generated entry and exit points, the resulting differences in trajectory lengths, the need to avoid convective weather areas, and the requirement to maintain conflict-free trajectories. Furthermore, as aircraft progress through successive planning horizons, their positions within the airspace change, affecting the initial states of subsequent horizons. Consequently, some aircraft may be close to their exit points at the beginning of a new planning horizon, whereas others may have only recently entered the airspace, leading to differences in the resulting total flight time.

When the flight trajectories obtained from the deterministic model are evaluated under different wind scenarios using the stochastic model, infeasibility may occur for some planning horizons. In such cases, the deterministic trajectories cannot satisfy the required aircraft separation constraints under all wind scenarios, and consequently, the corresponding z_v value cannot be calculated. These planning horizons also tend to require longer solution times in the stochastic model, as the increased potential for conflicts under different wind conditions makes the optimisation problem more complex. This indicates that solutions obtained without considering wind uncertainty may not be robust to variations in wind conditions. In contrast, the stochastic model provides feasible solutions for all planning horizons in the test problems, emphasising the importance of considering wind effects and handling the problem stochastically.

To further assess the operational impact of infeasibility, an additional analysis was performed for the cases where the VSS value could not be calculated due to the infeasibility of deterministic solutions under one or more wind scenarios. When a deterministic trajectory became infeasible under a wind scenario, additional operational manoeuvres, such as tactical rerouting, vectoring or airborne holding, would be required to restore conflict-free operations. These corrective actions may introduce additional delay, increased flight distance, fuel consumption and controller workload. In this study, the operational impact of such manoeuvres was represented by additional waiting time while preserving the fixed deterministic trajectories. For each test problem, the required waiting time was calculated for each wind scenario in which the deterministic solution became infeasible. The waiting times across these infeasible scenarios were then summed to obtain a cumulative recovery penalty. Scenario probabilities were not used in this calculation; therefore, the resulting value is interpreted as a descriptive recovery indicator rather than a probability-weighted expected operational cost. The obtained recovery penalties ranged from 21 s to 268 s, with an average value of approximately 109 s among the evaluated cases. Although the magnitude of the penalty varied depending on the traffic configuration, planning horizon and realised wind conditions, the results demonstrate that neglecting wind uncertainty could lead to additional operational adjustments after the realisation of uncertain conditions. Therefore, the stochastic approach provides not only improved robustness against wind uncertainty but also reduces the potential need for additional operational manoeuvres.

A VSS value of zero indicates that the deterministic and stochastic models yield the same total flight time for the corresponding planning horizon. For these planning horizons, the solution times of the stochastic model are notably short, with values below one minute. This can be attributed to the relatively small number of aircraft present in the initial planning horizons, which reduces the number of potential conflicts. In subsequent planning horizons, a large proportion of the aircraft have already completed their flights in previous horizons, which reduces the number of potential conflicts among the aircraft considered within the corresponding planning horizon.

The relationship between the number of aircraft and solution time is explored by Reference [33] that found an increase in the number of potential conflicts between aircraft increases problem complexity and extends the time required to reach an optimal solution. Furthermore, the growth and movement of

Downloaded from https://www.cambridge.org/core. 17 Nov 2026 at 23:48:34, subject to the Cambridge Core terms of use.

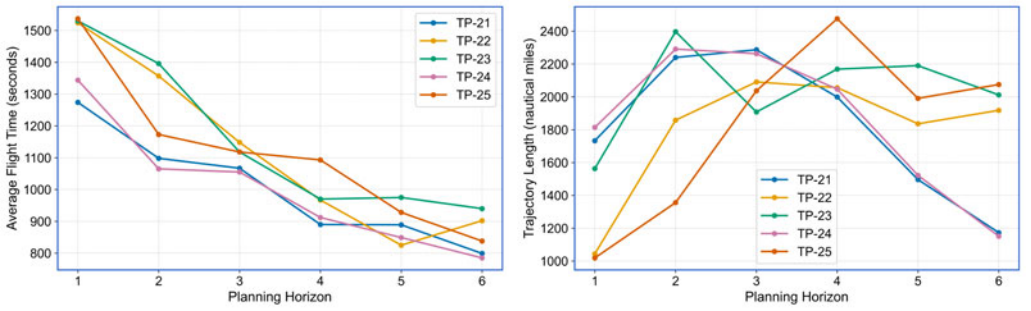


Figure 10. *Average flight times and trajectory lengths in CB-5 case.*

convective areas reduce the available airspace for trajectory planning, restricting the trajectory options for aircraft to avoid convective weather. This results in aircraft clustering in certain areas, increasing the probability of conflicts and making conflict resolution more complex due to the limited available airspace.

Figure 10 shows the trends in average flight time and trajectory length across planning horizons in the CB-5 case. As the planning horizon advances, an overall decrease in average flight time is observed. For instance, in TP-23, the average flight time drops significantly from 1,396 s in Horizon 2 to 1,118 s in Horizon 3 for the same number of aircraft, representing a reduction of 278 s.

In the initial horizons, the presence of large convective areas forces aircraft to follow longer, indirect trajectories around the southern regions of the airspace, particularly for flights from entry point 1 to exit point 5. Starting from Horizon 4, the opening of routes in the northeast enables shorter, more direct trajectories, resulting in a further reduction in flight times. For instance, between Horizons 3 and 4, the average flight times decrease by approximately 13.2–16.6% across all test problems except TP-25. In TP-25, the reduction is more moderate, with an observed decrease of 2.2% during the same interval. Furthermore, despite an increase in traffic density, the average flight time continues to decrease. These findings demonstrate the capability of the proposed optimisation model to adapt dynamically to changing airspace conditions, efficiently manage higher traffic densities and resolve potential conflicts.

Similarly, the trajectory length follows a comparable trend across the planning horizons. In the initial horizons, trajectory lengths generally increase due to the combined effects of higher traffic density and the need for more extensive rerouting to avoid large convective areas. From Horizon 3 onward, trajectory lengths decrease in most test problems as the convective areas gradually shrink and dissipate. This allows aircraft to follow more direct and efficient trajectories, particularly in the northeastern part of the airspace. The pronounced reduction in trajectory length observed from Horizon 4 onward in TP-21 and TP-24 can be attributed not only to the dissipation of the convective areas but also to the reduced number of aircraft within those planning horizons. Conversely, TP-22 and TP-23 exhibit greater variability during the later planning horizons. For example, the trajectory length in TP-23 decreases substantially in Horizon 3, increases again in Horizons 4 and 5, and then decreases in Horizon 6. These variations reflect the combined influence of the evolving convective weather, changes in traffic configuration and the conflict resolution manoeuvres.

Unlike the other test problems, TP-25 exhibits a distinct pattern in which the trajectory length gradually increases up to Horizon 4. This trend is primarily associated with increasing traffic density, which imposes additional conflict resolution constraints within the limited available airspace. Beyond Horizon 4, however, the trajectory length decreases and subsequently remains relatively stable despite the continued growth in traffic density. In contrast, the solution time increases progressively across the planning horizons. Although the dissipation of the convective areas increases the available airspace, the higher traffic density continues to increase the computational complexity of resolving potential conflicts. Nevertheless, the proposed optimisation model effectively handles both convective weather and conflict resolution requirements, producing optimal flight trajectories within computationally acceptable solution times.

Downloaded from https://www.cambridge.org/core. 17 Nov 2026 at 23:48:34, subject to the Cambridge Core terms of use.

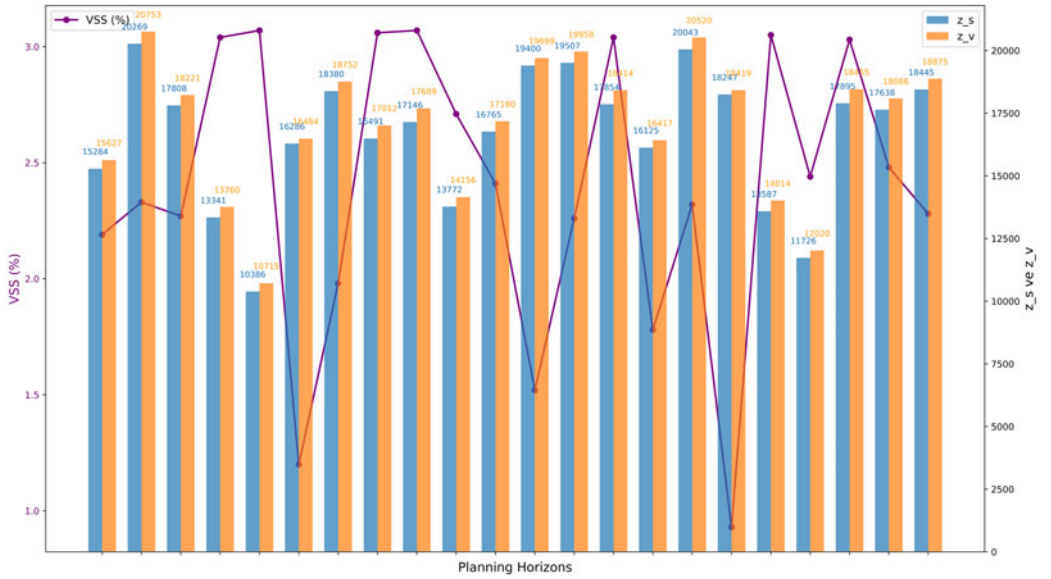


Figure 11. *Improvement rates achieved with the stochastic model for the CB-5 case.*

Figure 11 illustrates the results for the CB-5 case, showing the performance of both the stochastic and deterministic models across various planning horizons where the VSS value is positive. The graph compares the objective function values of the stochastic model (z_s) and the deterministic model (z_v), highlighting the operational improvements achieved through the stochastic approach. The VSS percentage, representing the relative enhancement in optimisation, varies between approximately 0.93 and 3.07% for the displayed planning horizons. Notably, a maximum absolute gain of 560 s in flight time (corresponding to VSS of 3.04%) was achieved for 19 aircraft.

VSS values ranged from 0% to 3.5% across the analysed convective weather cases, with some planning horizons resulting in a VSS of zero. A statistical analysis was performed on all 112 VSS (%) values, including planning horizons with VSS = 0. This analysis yielded a mean VSS of 1.95%, with a standard deviation of 0.98%. The corresponding 95% confidence interval for the mean VSS was estimated as [1.76%, 2.13%]. Since the lower bound of the confidence interval remains above zero, the results provide statistical evidence that considering wind uncertainty leads to an overall improvement over the deterministic approach across the analysed test problems. The distribution of VSS percentages across the CB cases, shown in Figure 12, further illustrates the influence of convective area evolution and airspace availability on the improvement achieved by the stochastic model. Cases with shrinking convective areas, such as CB-4 and CB-5, exhibit higher improvement rates due to increased available airspace, with mean values of 2.09% and 2.1%, respectively. In these cases, reducing convective areas over time allows for more efficient flight paths and better overall optimisation. Conversely, the CB-2 case, characterised by expanding convective areas, shows the lowest improvement rates, with a mean of 1.59%. The growing convective areas in this case restrict available airspace, making it more challenging to optimise flight paths and resulting in lower improvement rates. This analysis demonstrates the significant impact of airspace availability on the performance of the stochastic model and highlights the importance of considering dynamic weather conditions in ATM optimisation.

6.3. Sensitivity analysis

To further evaluate the proposed stochastic RHC framework, a sensitivity analysis was conducted to investigate the influence of both the number of wind scenarios and the assigned scenario probabilities. In addition to the wind scenarios presented in Table 2, an alternative nine-scenario set was generated,

Downloaded from https://www.cambridge.org/core. 17 Nov 2026 at 23:48:34, subject to the Cambridge Core terms of use.

Table 4. *Nine wind scenarios and probabilities*

Scenarios	Direction	Speed	Probability (%)
s1	195	39	9.3
s2	195	59	14
s3	195	79	9.3
s4	255	39	7.1
s5	255	59	20.9
s6	255	79	25.6
s7	255	99	4.6
s8	255	119	4.6
s9	315	39	4.6

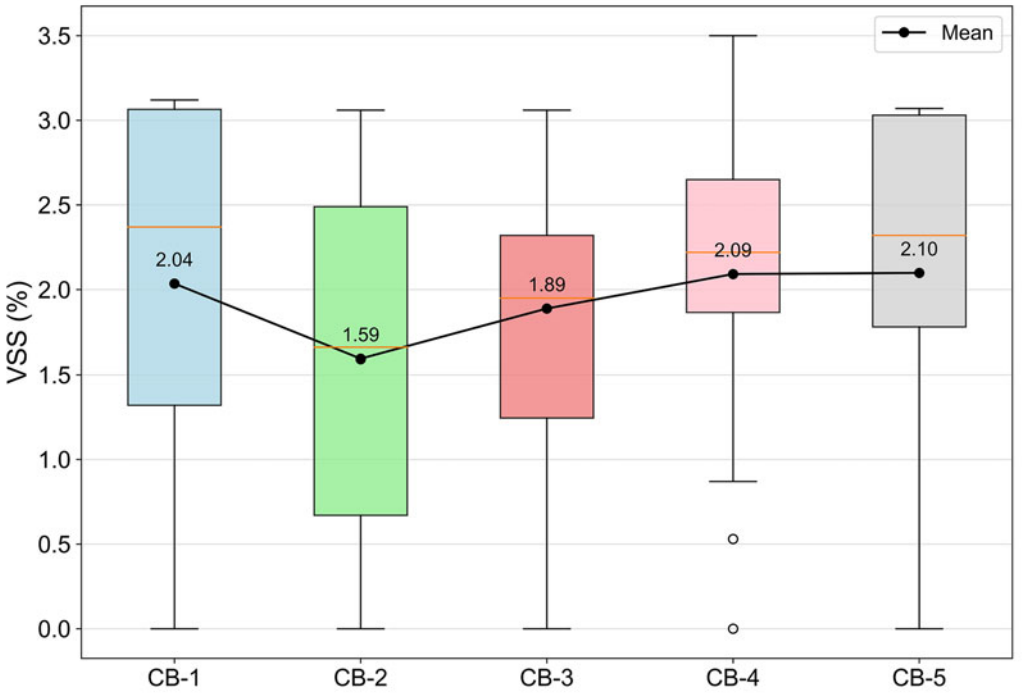


Figure 12. *Comparison of VSS improvement for all CB cases.*

and the corresponding scenario probabilities are reported in Table 4. Furthermore, the five-scenario configuration was also evaluated by assigning equal probabilities to all scenarios. The results of the sensitivity analysis are presented in Table 5, where the solution time and VSS values for each test problem represent the averages across all planning horizons within that problem, while the last row presents the overall averages across all test problems.

Using the five-scenario configuration with empirical probabilities as the reference, both the equal probability and the nine-scenario configurations produced changes in the VSS values. Under the equal probability configuration, the average VSS (%) increased for TP-21, TP-22, TP-23 and TP-24, whereas it decreased for TP-25. Similarly, the nine-scenario configuration resulted in higher VSS (%) values for TP-21, TP-23 and TP-25, while lower values were observed for TP-22 and TP-24. Despite these variations at the individual test problem level, the overall average VSS (%) remained remarkably stable across all three configurations, with values of 2.10%, 2.11% and 2.16% for the reference five-scenario configuration, the equal probability configuration, and the nine-scenario configuration, respectively.

Downloaded from https://www.cambridge.org/core. 17 Nov 2026 at 23:48:34, subject to the Cambridge Core terms of use.

Table 5. *Results of the sensitivity analysis*

	Five scenarios (reference)			Five scenarios (equal probability)			Nine scenarios		
Test problem	Solution time	VSS	VSS (%)	Solution time	VSS	VSS (%)	Solution time	VSS	VSS (%)
TP-21	109	397	2.58	71	385	2.65	440	462	2.90
TP-22	81	327	1.86	71	348	2.01	374	315	1.78
TP-23	196	422	2.39	100	434	2.55	514	442	2.49
TP-24	107	274	1.62	82	319	1.93	297	253	1.37
TP-25	144	346	2.05	120	236	1.43	325	396	2.25
Average	127	353	2.10	89	344	2.11	390	373	2.16

Downloaded from https://www.cambridge.org/core. 17 Nov 2026 at 23:48:34, subject to the Cambridge Core terms of use.

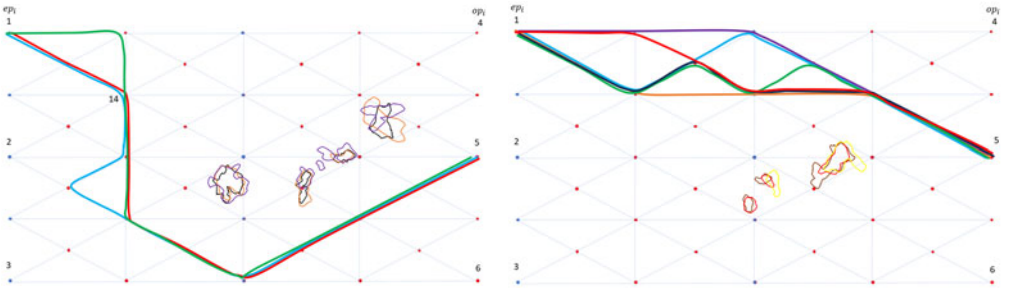


Figure 13. *Flight trajectories before and after convective weather dissipation in the CB-5 case.*

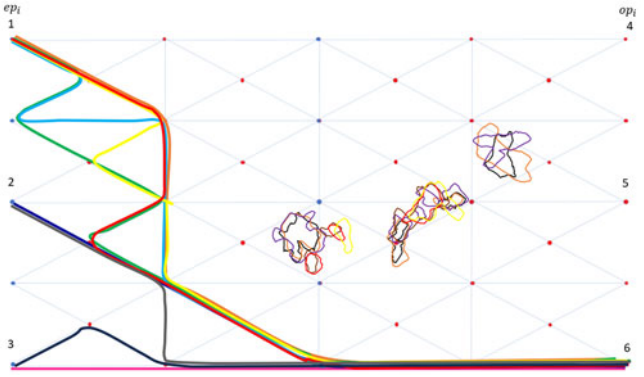


Figure 14. *Conflict resolution trajectories in the CB-5 case.*

The computational performance, however, exhibited a more noticeable dependence on the scenario configuration. The equal probability configuration reduced the average solution time from 127 s to 89 s, whereas increasing the number of scenarios from five to nine increased the average solution time substantially from 127 s to 390 s. These findings suggest that increasing the number of wind scenarios results in only a marginal increase in the average VSS (%) while substantially increasing the computational effort.

6.4. Assessment of flight trajectories

This section examines the evolution of flight trajectories across successive planning horizons for the CB-5 case. Figures 13 and 14 present representative trajectory examples illustrating the adaptation of aircraft routeing to convective weather evolution and the resolution of aircraft conflicts while maintaining the required separation. Additional trajectory examples illustrating different conflict resolution and weather adaptation behaviours, together with their corresponding descriptions, are provided in Appendix C (Figures 15–17).

Figure 13 presents the trajectories for aircraft operating from entry point 1 to exit point 5. Figure 13(a) shows the trajectories generated during planning horizons 1–3, when severe convective cells obstruct the central and northeastern parts of the airspace. Under these conditions, the red trajectory represents the shortest feasible trajectory around the convective areas, while the green and blue trajectories correspond to conflict-resolution manoeuvres introduced to maintain the required separation. Figure 13(b) shows the trajectories generated during planning horizons 4–6. As the convective areas in the northeastern sector gradually dissipate, additional airspace becomes available, enabling aircraft to follow shorter trajectories through the northern part of the airspace. Due to the overlapping structure of the RHC framework, aircraft assigned to the southern trajectories during planning horizon 3 that had not yet passed waypoint 14 are reoptimised at planning horizon 4 and reassigned to the newly available northern trajectories.

Downloaded from https://www.cambridge.org/core. 17 Nov 2026 at 23:48:34, subject to the Cambridge Core terms of use.

Figure 14 presents the trajectories of aircraft operating from entry points 1, 2, and 3 and sharing a common destination at exit point 6. These trajectories are generated as part of the simultaneous optimisation of all aircraft operating within the airspace. Aircraft entering from entry point 3 generally follow the shortest feasible trajectory along the southern boundary. In contrast, aircraft entering from 1 and 2 are assigned longer trajectories involving lateral deviations to maintain the required separation while merging with the surrounding traffic. As illustrated by the cyan, green and yellow trajectories in the western part of the airspace, these lateral deviations increase the trajectory length to provide the temporal spacing required for conflict-free operations while avoiding the convective weather.

7. Discussion and conclusion

In this study, mathematical models were proposed to avoid convective areas and resolve potential conflicts between aircraft during en-route flights in the airspace. To achieve this, two different models were developed: one based on a deterministic approach and the other using two-stage stochastic programming considering wind direction and speed uncertainties. The objective of these models is to minimise the total flight time of the aircraft while determining the flight trajectories between the entry and exit points. An RHC framework was also applied to consider the dynamic behaviour of convective areas. Five different convective area cases were created to test the models, with five randomly generated test problems for each case.

Our results show that the stochastic model consistently provides better, or equal, solutions compared to the deterministic model under wind uncertainties and provides optimal solutions for all planning horizons in each convective area case. To further evaluate the advantages of the stochastic model, its effectiveness was assessed using the VSS metric, which quantifies the benefits gained over the deterministic approach. In some scenarios, a VSS of zero was obtained, indicating identical performance between the models. Meanwhile, positive VSS values ranging from 0.4 to 3.5% demonstrate the operational benefits of incorporating wind uncertainty into the proposed stochastic RHC framework. Positive VSS values indicate improvements in the flight time objective resulting from explicitly accounting for wind uncertainty. Because flight time is directly included in the objective function, a positive VSS represents an improvement in total flight-time efficiency relative to the deterministic formulation. The maximum absolute improvement reached 560 s in total flight time for a planning horizon involving 19 aircraft within the 120 NM $\times$ 120 NM modelled airspace at a single flight level. Furthermore, the statistical analysis of VSS values yielded a mean VSS of 1.95%, with a 95% confidence interval of [1.76%, 2.13%], providing statistical evidence that the stochastic framework consistently outperforms the deterministic approach for the analysed test problems. The additional sensitivity analysis further showed that the average VSS remained largely unchanged under different scenario probability assignments and increased only marginally when the number of representative wind scenarios was increased from five to nine, despite a substantial increase in computational effort.

The application of the RHC framework to the proposed stochastic model requires a state propagation approximation. When transitioning to the next planning horizon, each aircraft that has not exited the airspace is initialised at the trajectory point closest to its position at the end of the current horizon. The corresponding start time is determined from a reference scenario selected using a probability-based roulette wheel method, rather than propagating the full distribution of possible start times. This approximation is adopted to avoid the exponential growth of the scenario tree and ensure computational tractability.

When state propagation is performed using a reference scenario, aircraft transferred from the previous planning horizon are initialised under the selected wind scenario, thereby maintaining their relative temporal relationships during the transition. Furthermore, the overlapping RHC approach allows aircraft trajectories near the horizon boundary to be reconsidered in subsequent planning horizons. At the beginning of each subsequent planning horizon, the stochastic optimisation model is updated with the complete set of wind scenarios and the latest convective weather information, while considering both aircraft transferred from the previous planning horizon and newly entering aircraft. This enables the model to incorporate updated uncertainty information and limits the impact of the

Downloaded from https://www.cambridge.org/core. 17 Nov 2026 at 23:48:34, subject to the Cambridge Core terms of use.

state propagation approximation over consecutive planning horizons. In addition, the positive VSS values indicate that considering wind uncertainty within each planning horizon provides benefits over the corresponding deterministic formulation, supporting the effectiveness of the stochastic approach. Therefore, although the state propagation between horizons represents a modelling approximation, the proposed approach can generate operationally meaningful and practically useful plans under evolving convective weather conditions.

The results showed that the stochastic model consistently provided feasible flight trajectories for all defined planning horizons under varying wind scenarios. In contrast, the deterministic model failed to produce applicable flight trajectories, i.e. not feasible in terms of operations, under wind uncertainties in some scenarios due to its inability to adapt to changes in wind conditions. This highlights a critical drawback of deterministic models in scenarios with significant environmental uncertainties. The inflexibility of deterministic routeing often results in infeasible decisions, requiring ATCOs to reroute aircraft when uncertainties arise. This results in increased controller workload. As a result, our findings suggest that the stochastic model developed in this study may provide better decision support for ATCOs compared to the deterministic approach.

Convective area cases exhibited various characteristics, with some areas growing and others shrinking over time. These changes affected the available airspace, which influenced the optimisation of flight routes. Increased available airspace allowed for more efficient routeing and reduced flight times, while reduced airspace due to growing convective areas led to increased potential conflicts and longer routes.

The models are developed with general airspace, making them adaptable as decision support systems in several convective weather conditions. The deterministic model may increase the workload for ATCOs due to the need for rerouting when its solutions fail under uncertainty. In contrast, the stochastic model provides robust solutions that do not require rerouting. In addition, the shorter flight times achieved by the models increase fuel efficiency. Therefore, it can reduce the environmental impact through less fuel consumption.

This study demonstrates the importance of considering dynamic weather conditions and wind uncertainties in ATM. The proposed models enhance the safety and efficiency of en-route flights and provide valuable insights for pilots and ATCOs in planning and managing flight trajectories under convective weather conditions.

8. Limitations and future work

The proposed approach ensures safe separation using an airspace discretisation technique that allows focusing on critical points known as potential conflict points including entry, exit and route intersections, rather than searching the entire airspace. However, it does not explicitly specify how aircraft perform manoeuvres at these points, especially when turns are required. At these critical points, aircraft may perform a fly-by turn consisting of a coordinated turn, as suggested in Reference [1], although other types of manoeuvres may be applicable depending on the operational context. These may include vector techniques, fly-over turns, speed changes or more complex combinations of manoeuvres, influenced by airspace structure, traffic conditions and aircraft capabilities. Since operational constraints such as aircraft performance limitations, manoeuvring capabilities and regulatory guidelines may affect the practical feasibility of some of the generated trajectories, an appropriate manoeuvre strategy should be clearly defined to ensure operational applicability. Nevertheless, the proposed model generates conflict-free flight trajectories that are consistent with typical en-route operations and comply with standard separation requirements, suggesting a high degree of operational feasibility. The existing model can be combined with a predefined manoeuvre strategy, which can be integrated into the framework to ensure that planned trajectories are consistent with aircraft capabilities and allow for more strategic and realistic flight planning.

In this study, all operations are considered at a single flight level. There are several reasons for adopting this approach. First, in the presence of convective weather events such as thunderstorms, changing altitude does not necessarily guarantee avoidance, as these weather systems often occupy multiple flight levels with different spatial extent [37, 52]. Secondly, when convective weather restricts the available

Downloaded from https://www.cambridge.org/core. 17 Nov 2026 at 23:48:34, subject to the Cambridge Core terms of use.

airspace, changing the assigned altitude of one aircraft may cause additional potential conflicts with other aircraft operating at higher or lower flight levels. Furthermore, altitude changes are generally avoided due to passenger discomfort, increased fuel consumption and the difficulty for controllers to monitor altitude-based manoeuvres [20]. For these reasons, pilots and air traffic controllers generally prefer horizontal manoeuvres, which provide more flexibility, lower fuel consumption, time savings and improved safety in en-route operations [37].

While the focus on two-dimensional trajectories is justified by various operational and safety considerations, this assumption inherently introduces certain limitations. Specifically, restricting the model to a single flight level reduces the degrees of freedom available in the optimisation process. Theoretically, allowing vertical manoeuvres would expand the solution space and provide aircraft with additional options for conflict resolution. This could reduce total flight time and improve the objective function value. Consequently, the exclusion of altitude changes may result in some loss of potential optimisation benefits. However, this represents a trade-off between optimisation potential and operational feasibility, as the use of vertical manoeuvres could lead to additional fuel consumption, increased ATC workload and operational complexity. Although the exclusion of altitude changes is consistent with the operational assumptions considered in this study, it may limit the model's ability to address highly complex or severely congested airspace scenarios. In such contexts, vertical manoeuvres may provide an additional means of resolving conflicts and avoiding dynamic convective weather systems. In future work, the model can be extended to include altitude changes, allowing aircraft to move between flight levels as required. This would improve the adaptability of the model and enable more strategic and flexible three-dimensional trajectory planning in complex airspace environments.

Another limitation of the proposed framework is the assumption of a spatially uniform upper-air wind field over the modelled airspace. Localised spatial variations in wind speed and direction are not represented within the proposed optimisation framework. Consequently, the reported results reflect the influence of the prevailing upper-air wind conditions in the modelled airspace rather than localised variability. The derived wind scenarios are specific to the meteorological characteristics of the Istanbul region and therefore cannot be directly transferred to other geographical regions. However, the proposed stochastic framework is not geographically restricted; its application to other regions would require representative local upper-air observations and the corresponding reconstruction of the wind scenarios and their probabilities. Future research should investigate the influence of spatially varying upper-air wind fields on trajectory optimisation.

Furthermore, the proposed model is developed based on the airspace discretisation technique and has been implemented with a certain number of waypoints. As pointed out by Reference [33], increasing the discretisation rate leads to a significant increase in solution time without providing an equivalent improvement in solution quality. Similarly, a certain number of entry and exit points were selected to represent diverse routeing possibilities while maintaining a balance between routeing flexibility and computational efficiency.

To allow aircraft to change altitude, the model would need to be restructured to consider multiple flight levels and allow vertical movement. However, the inclusion of this additional dimension would significantly reduce computational efficiency, especially when a larger number of aircraft are operating simultaneously at multiple flight levels. Similarly, larger airspace configurations or higher traffic densities would increase the number of candidate trajectories and potential aircraft–aircraft interactions, thereby increasing the computational burden of the optimisation problem. As the size of the problem increases, the time required to obtain a solution increases substantially, making it more difficult to obtain optimal solutions within a reasonable time frame. To improve the scalability of the proposed framework to larger and more complex airspace configurations, future research could investigate heuristic or meta-heuristic solution approaches that can obtain high-quality near-optimal solutions with lower computational effort.

Furthermore, a limitation of the proposed RHC framework is that temporal states are propagated between consecutive planning horizons using a reference scenario selected through a probability-based roulette wheel method, rather than the full distribution of possible states. Although this approximation is necessary to maintain computational tractability, it may not fully capture the evolution of temporal

Downloaded from https://www.cambridge.org/core. 17 Nov 2026 at 23:48:34, subject to the Cambridge Core terms of use.

uncertainty across consecutive planning horizons. Nevertheless, the positive VSS results, together with the repeated stochastic re-optimisation performed at each overlapping planning horizon, suggest that the proposed framework remains practically useful despite this approximation. However, the specific effect of the reference scenario state propagation approximation on solution quality has not been quantified in the present study. Future research could investigate alternative state propagation strategies, such as multi-scenario state propagation or scenario reduction techniques, to better preserve the evolution of temporal uncertainty across planning horizons while maintaining computational efficiency.

Declaration of competing interest. The authors declare that they have no known competing financial interests or personal relationships that could have appeared to influence the work reported in this paper.

Declaration of generative AI and AI-assisted technologies in the writing process. During the preparation of this work the author(s) used AI to improve language and readability, with caution. After using an AI tool, the author(s) reviewed and edited the content as needed and take(s) full responsibility for the content of the publication.

References

[1] Kaplan, Z., Çetek, C. and Saraç, T. A multi-objective nonlinear integer programming model for mixed runway operations within the TMAs, *Aeronaut. J.*, 2024, **128**, pp 340–370. https://doi.org/10.1017/aer.2023.50

[2] SESAR. SESAR Joint Undertaking | A new dawn for weather-resilient air traffic management. 2023, January 17. https://www.sesarju.eu/news/new-dawn-weather-resilient-air-traffic-management0

[3] EUROCONTROL. Aviation's summer impacted by the weather, 2023a. https://www.eurocontrol.int/press-release/aviations-summer-impacted-weather

[4] EUROCONTROL. Making operations more predictable during adverse weather, 2023b. https://www.eurocontrol.int/news/making-operations-more-predictable-during-adverse-weather

[5] Allen, J.T. Climate Change and Severe Thunderstorms, *Oxford Research Encyclopedia of Climate Science*. Oxford University Press, 2018. https://doi.org/10.1093/acrefore/9780190228620.013.62

[6] Brooks, H.E. Severe thunderstorms and climate change, *Atmos. Res.*, 2013, **123**, pp 129–138. https://doi.org/10.1016/j.atmosres.2012.04.002

[7] Haberlie, A.M., Ashley, W.S., Battisto, C.M. and Gensini, V.A. Thunderstorm activity under intermediate and extreme climate change scenarios, *Geophys. Res. Lett.*, 2022, **49**, p e2022GL098779. https://doi.org/10.1029/2022GL098779

[8] Raupach, T.H., Martius, O., Allen, J.T., Kunz, M., Lasher-Trapp, S., Mohr, S., Rasmussen, K.L., Trapp, R.J. and Zhang, Q. The effects of climate change on hailstorms, *Nat. Rev. Earth Environ.*, 2021, **2**, pp 213–226. https://doi.org/10.1038/s43017-020-00133-9

[9] Airbus. Optimum use of weather radar, 2016.

[10] Administration, F.A. Advisory circular - thunderstorms - AC 00-24C, 2013. http://www.faa.gov/regulations_policies/advisory_circulars/

[11] ICAO, 8.6.9. Information Regarding Adverse Weather, *Doc 4444 - Air Traffic Management Procedures for Air Navigation Services*, 2016a.

[12] ICAO, *15.2.3. Weather deviation procedures. In Doc 4444 - Air Traffic Management Procedures for Air Navigation Services*, 2016b.

[13] Trier, S.B. and Sharman, R.D. Convection-permitting simulations of the environment supporting widespread turbulence within the upper-level outflow of a mesoscale convective system, *Mon. Weather Rev.*, 2009, **137**, pp 1972–1990. https://doi.org/10.1175/2008MWR2770.1

[14] Rubnich, M. and Delaura, R. An Algorithm to Identify Robust Convective Weather Avoidance Polygons in En Route Airspace. 10th AIAA Aviation Technology, Integration, and Operations (ATIO) Conference, 2010, September 13.

[15] Cecen, R.K. and Cetek, C. Conflict-free en-route operations with horizontal resolution manoeuvers using a heuristic algorithm, *Aeronaut. J.*, 2020, **124**, pp 767–785. https://doi.org/10.1017/aer.2020.5

[16] Cecen, R.K. and Cetek, C. A two-step approach for airborne delay minimization using pretactical conflict resolution in free-route airspace, *J. Adv. Transp.*, 2019, **2019**, 4805613, 17 pages. https://doi.org/10.1155/2019/4805613

[17] Cecen, R.K., Saraç, T. and Cetek, C. Meta-heuristic algorithm for aircraft pre-tactical conflict resolution with altitude and heading angle change maneuvers, *TOP*, 2021, **29**, pp 629–647. https://doi.org/10.1007/s11750-020-00585-8

[18] Cafieri, S. and Durand, N. Aircraft deconfliction with speed regulation: new models from mixed-integer optimization, *J. Glob. Optim.*, 2014, **58**, pp 613–629. https://doi.org/10.1007/s10898-013-0070-1

[19] Cafieri, S. and Rey, D. Maximizing the number of conflict-free aircraft using mixed-integer nonlinear programming, *Comput. Op. Res.*, 2017, **80**, pp 147–158. https://doi.org/10.1016/j.cor.2016.12.002

[20] Omer, J. A space-discretized mixed-integer linear model for air-conflict resolution with speed and heading maneuvers, *Comput. Oper. Res.*, 2015, **58**, pp 75–86. https://doi.org/10.1016/j.cor.2014.12.012

[21] Vela, A., Solak, S., Singhose, W. and Clarke, J.P. A mixed integer program for flight-level assignment and speed control for conflict resolution, *Proceedings of the IEEE Conference on Decision and Control*, 2009, pp 5219–5226. https://doi.org/10.1109/CDC.2009.5400520

[22] Alonso-Ayuso, A., Escudero, L.F. and Martín-Campo, F.J. A mixed 0-1 nonlinear optimization model and algorithmic approach for the collision avoidance in ATM: velocity changes through a time horizon, *Comput. Op. Res.*, 2012, **39**, pp 3136–3146. https://doi.org/10.1016/j.cor.2012.03.015

Downloaded from https://www.cambridge.org/core. 17 Nov 2026 at 23:48:34, subject to the Cambridge Core terms of use.

[23] Alonso-Ayuso, A., Escudero, L.F. and Martín-Campo, F.J. Exact and approximate solving of the aircraft collision resolution problem via turn changes, *Transp. Sci.*, 2014, **50**, pp 263–274. https://doi.org/10.1287/trsc.2014.0557
[24] Cafieri, S. and Omheni, R. Mixed-integer nonlinear programming for aircraft conflict avoidance by sequentially applying velocity and heading angle changes, *Eur. J. Op. Res.*, 2017, **260**, pp 283–290. https://doi.org/10.1016/j.ejor.2016.12.010
[25] Christodoulou, M. and Costoulakis, C. Nonlinear mixed integer programming for aircraft collision avoidance in free flight, *ceedings of the Mediterranean Electrotechnical Conference - MELECON*, 2004, **1**, pp 327–330. https://doi.org/10.1109/MELCON.2004.1346858
[26] Pallottino, L., Feron, E.M. and Bicchi, A. Conflict resolution problems for air traffic management systems solved with mixed integer programming, *IEEE Trans. Intell. Transp.*, 2002, **3**, pp 3–11. https://doi.org/10.1109/6979.994791
[27] Vela, A.E., Solak, S., Clarke, J.P.B., Singhose, W.E., Barnes, E.R. and Johnson, E.L. Near real-time fuel-optimal en route conflict resolution, *IEEE Trans. Intell. Transp.*, 2010, **11**, pp 826–837. https://doi.org/10.1109/TITS.2010.2051028
[28] Alonso-Ayuso, A., Escudero, L.F. and Martín-Campo, F.J. Collision avoidance in air traffic management: a mixed-integer linear optimization approach, *IEEE Trans. Intell. Transp. Syst.*, 2011, **12**, pp 47–57. https://doi.org/10.1109/TITS.2010.2061971
[29] Alonso-Ayuso, A., Escudero, L.F., Olaso, P. and Pizarro, C. Conflict avoidance: 0-1 linear models for conflict detection and resolution, *TOP*, 2011, **21**, pp 485–504. https://doi.org/10.1007/s11750-011-0224-6
[30] Alonso-Ayuso, A., Escudero, L.F. and Martín-Campo, F.J. Multiobjective optimization for aircraft conflict resolution. A metaheuristic approach, *Eur. J. Op. Res.*, 2016, **248**, pp 691–702. https://doi.org/10.1016/j.ejor.2015.07.049
[31] Erzberger, H. and Heere, K. Algorithm and operational concept for resolving short-range conflicts, *Proceedings of the Institution of Mechanical Engineers, Part G: Journal of Aerospace Engineering*, 2010, **224**, pp 225–243. https://doi.org/10.1243/09544100JAERO546
[32] Hong, Y., Choi, B., Oh, G., Lee, K. and Kim, Y. Nonlinear conflict resolution and flow management using particle swarm optimization, *IEEE Trans. Intell. Transp. Syst.*, 2017, **18**, pp 3378–3387. https://doi.org/10.1109/TITS.2017.2684824
[33] Kaplan, Z., Çetek, C. and Saraç, T. A mixed-integer linear programming model for conflict resolution using airspace discretization technique in a generic free route airspace, *J. Polytech.*, 2024, **27**, pp 1427–1440. https://doi.org/10.2339/politeknik.1293137
[34] NG, K. K. H. Emission-Aware adjustable robust flight path planning with respect to fuel and contrail cost, *Transp. B*, 2022, **11**, pp 24–68. https://doi.org/10.1080/21680566.2022.2036651
[35] Kamo, S., Rosenow, J., Fricke, H. and Soler, M. Robust optimization integrating aircraft trajectory and sequence under weather forecast uncertainty, *Transp. Res. Part C: Emerg. Technol.*, 2023, **152**, p 104187. https://doi.org/10.1016/J.TRC.2023.104187
[36] Seenivasan, D.B., Olivares, A. and Staffetti, E. Multi-aircraft optimal 4D online trajectory planning in the presence of a multi-cell storm in development, *Transp. Res. Part C: Emerg. Technol.*, 2020, **110**, pp 123–142. https://doi.org/10.1016/j.trc.2019.11.014
[37] Hauf, T., Sakiew, L. and Sauer, M. Adverse weather diversion model DIVMET, *J. Aerosp. Op.*, 2013, **2**, pp 115–133. https://doi.org/10.3233/aop-130037
[38] Schilke, C. and Hecker, P. Dynamic route optimization based on adverse weather data. SIDs 2014 - Proceedings of the SESAR Innovation Days, November, 2014.
[39] Xie, Z. and Zhong, Z.W. Aircraft path planning under adverse weather conditions, *MATEC Web of Conferences*, 2016. https://doi.org/10.1051/(2016).
[40] González-Arribas, D., Hentzen, D., Sanjurjo-Rivo, M., Soler, M. and Kamgarpour, M. Optimal aircraft trajectory planning in the presence of stochastic convective weather cells, *17th AIAA Aviation Technology, Integration, and Operations Conference*, 2017. https://doi.org/10.2514/6.2017-3431
[41] Andrés, E., González-Arribas, D., Soler, M., Kamgarpour, M., Sanjurjo-Rivo, M. and Simarro, J. Iterative graph deformation for aircraft trajectory planning considering ensemble forecasting of thunderstorms, *Transp. Res. Part C: Emerg. Technol.*, 2022, **145**, p 103919. https://doi.org/10.1016/j.trc.2022.103919
[42] Hentzen, D., Kamgarpour, M., Soler, M. and González-Arribas, D. On maximizing safety in stochastic aircraft trajectory planning with uncertain thunderstorm development, *Aerosp. Sci. Technol.*, 2018, **79**, pp 543–553. https://doi.org/10.1016/j.ast.2018.06.006
[43] Franco, A., Rivas, D. and Valenzuela, A. *Optimal Aircraft Path Planning in a Structured Airspace Using Ensemble Weather Forecasts*, SESAR Innovation Days, 2018, *December*, Salzburg, Austria.
[44] Lindner, M., Rosenow, J., Zeh, T. and Fricke, H. In-flight aircraft trajectory optimization within corridors defined by ensemble weather forecasts, *Aerospace*, 2020, **7**, pp 1–18. https://doi.org/10.3390/aerospace7100144
[45] Taylor, C., Liu, S., Wanke, C. and Stewart, T. Generating diverse reroutes for tactical constraint avoidance, *J. Air Transp.*, 2018, **26**, pp 49–59. https://doi.org/10.2514/1.D0089
[46] Pang, Y., Zhao, X., Yan, H. and Liu, Y. Data-driven trajectory prediction with weather uncertainties: a Bayesian deep learning approach, *Transp. Res. Part C: Emerg. Technol.*, 2021, **130**, p 103326. https://doi.org/10.1016/j.trc.2021.103326
[47] Liu, W. and Hwang, I. Probabilistic aircraft midair conflict resolution using stochastic optimal control, *IEEE Trans. Intell. Transp.*, 2014, **15**, pp 37–46. https://doi.org/10.1109/TITS.2013.2274999
[48] Zhou, Y., Hu, M., Delahaye, D. and Yang, L. Multi-objective four-dimensional trajectory planning for free-route operations considering weather forecast uncertainty, *J. Air Transp. Manag.*, 2025, **128**, p 102831. https://doi.org/10.1016/J.JAIRTRAMAN.2025.102831.
[49] Pannequin, J.J., Bayen, A.M., Mitchell, I.M., Chung, H. and Sastry, S. Multiple aircraft deconflicted path planning with weather avoidance constraints, *AIAA Guidance, Navigation and Control Conference and Exhibit*, 2007, August 20.

Downloaded from https://www.cambridge.org/core. 17 Nov 2026 at 23:48:34, subject to the Cambridge Core terms of use.

[50] Erzberger, H., Lauderdale, T.A. and Chu, Y.C. Automated conflict resolution, arrival management, and weather avoidance for air traffic management, *Proc. Inst. Mech. Eng., Part G: J. Aerosp. Eng.*, 2012, **226**, pp 930–949. https://doi.org/10.1177/0954410011417347

[51] Clarke, J.P.B., Solak, S., Chang, Y.H., Ren, L. and Vela, A.E. Air traffic flow management in the presence of uncertainty, *Proceedings of the 8th USA/Europe Air Traffic Management Research and Development Seminar*, 2009, pp 571–580.

[52] Kamgarpour, M., Dadok, V. and Tomlin, C. Trajectory generation for aircraft subject to dynamic weather uncertainty, *Proceedings of the IEEE Conference on Decision and Control*, 2010, pp 2063–2068. https://doi.org/10.1109/CDC.2010.5717889

[53] Akdogan, F. and Sahin, A.D. A survey of route optimisation and planning based on meteorological conditions, *Aeronaut J.*, 2025, **130**, pp 613–638. https://doi.org/10.1017/aer.2025.10075

[54] Rathnakumar, R. and Liu, Y. Towards safer general aviation operations using a vision-based decision support system for weather threat avoidance, *J. Air Transp. Manag.*, 2025, **123**, p 102709. https://doi.org/10.1016/j.jairtraman.2024.102709

[55] Ertem, M., Ozcelik, F. and Saraç, T. Single machine scheduling problem with stochastic sequence-dependent setup times, *Int. J. Prod. Res.*, 2019, **57**, pp 3273–3289. https://doi.org/10.1080/00207543.2019.1581383

[56] Ozcelik, F., Ertem, M. and Saraç, T. A stochastic approach for the single-machine scheduling problem to minimize total expected cost with client-dependent tardiness costs, *Eng. Optim.*, 2022, **54**, pp 1178–1192. https://doi.org/10.1080/0305215X.2021.1919098

[57] Cecen, R.K., Cetek, C. and Kaya, O. Aircraft sequencing and scheduling in TMAs under wind direction uncertainties, *Aeronaut. J.*, 2020, **124**, pp 1896–1912. https://doi.org/10.1017/aer.2020.68

[58] Birge, J.R. and Louveaux, F. Introduction to Stochastic Programming T. In Mikosch, V., Resnick, S.I. and Robinson, S.M. (Eds), Second Edition, Springer, 2011. http://www.springer.com/series/3182

[59] Dönmez, K., Çetek, C. and Kaya, O. Air traffic management in parallel-point merge systems under wind uncertainties, *J. Air Transp. Manag.*, 2022, **104**, p 102268. https://doi.org/10.1016/j.jairtraman.2022.102268

[60] Dantzig, G.B. Linear Programming under Uncertainty. 1995, 1(3-4), 197–206. https://doi.org/10.1287/MNSC.1.3-4.197

[61] Kaya, O., Bagci, F. and Turkay, M. Planning of capacity, production and inventory decisions in a generic reverse supply chain under uncertain demand and returns, *Int. J. Prod. Res.*, 2014, **52**, pp 270–282. https://doi.org/10.1080/00207543.2013.838330

[62] Shapiro, A. and Philpott, A. A tutorial on stochastic programming, 2007.

[63] Saraç, T., Ozcelik, F. and Ertem, M. Unrelated parallel machine scheduling problem with stochastic sequence dependent setup times, *Op. Res.*, 2023, **23**, pp 1–19. https://doi.org/10.1007/s12351-023-00789-3

[64] Turkish State Meteorological Service. Meteorological Data Information Sales and Presentation System (MEVBİS), 2023. https://mevbis.mgm.gov.tr/mevbis/ui/index.html#/Workspace

[65] Meteomanz.com. Weather data SYNOPS/BUFR - GFS/ECMWF forecast, 2023. http://meteomanz.com/index?l=1

[66] University, I.S. Iowa Environmental Mesonet, 2023. https://mesonet.agron.iastate.edu/request/download.phtml?network=TR__ASOS#

[67] Weatherdata. University of Wyoming College of Engineering, 2023. https://weather.arcc.uwyo.edu/upperair/sounding.shtml

[68] Propoi, A.I. Use of linear programming methods for synthesizing sampled data automatic systems, *Automn. Remote Control*, 1963, **24**, pp 837–844. https://doi.org/10.11509/ISCIESCI.46.5_286

[69] Zadeh, L. and Whalen, B. On optimal control and linear programming, *IRE Trans. Autom. Control*, 1962, **7**, pp 45–46.

[70] Mayne, D.Q., Rawlings, J.B., Rao, C.V. and Scokaert, P.O.M. Constrained model predictive control: stability and optimality, *Automatica*, 2000, **36**, pp 789–814. https://doi.org/10.1016/S0005-1098(99)00214-9

[71] Lieder, A. and Stolletz, R. Scheduling aircraft take-offs and landings on interdependent and heterogeneous runways, *Transp. Res. Part E: Logist. Transp. Rev.*, 2016, **88**, pp 167–188. https://doi.org/10.1016/j.tre.2016.01.015

[72] Samà, M., D'Ariano, A. and Pacciarelli, D. Rolling horizon approach for aircraft scheduling in the terminal control area of busy airports, *Transp. Res. Part E: Logist. Transp. Rev.*, 2013, **60**, pp 140–155. https://doi.org/10.1016/j.tre.2013.05.006

[73] De Schutter, B. and Van Den Boom, T. Model predictive control for max-plus-linear discrete event systems, *Automatica*, 2001, **37**, pp 1049–1056.

[74] Furini, F., Persiani, C.A. and Toth, P. Aircraft Sequencing Problems via a Rolling Horizon Algorithm, Combinatorial Optimization: Second International Symposium, ISCO, 2012,

[75] Van Den Boom, T. and De Schutter, B. Properties of MPC for max-plus-linear systems, *Eur. J. Control*, 2002, **8**, pp 453–462.

[76] Krozel, J. Survey of weather impact models used in air traffic management, *10th AIAA Aviation Technology, Integration and Operations Conference 2010, ATIO*, 2010, **1**, pp 1–24. https://doi.org/10.2514/6.2010-9020

[77] Matthews, M.P. and Delaura, R. Assessment and interpretation of en route weather avoidance fields from the convective weather avoidance model, *10th AIAA Aviation Technology, Integration and Operations Conference 2010, ATIO*, 2010, **2010**, p 2. https://doi.org/10.2514/6.2010-9160.

[78] Summers, S., Kamgarpour, M., Tomlin, C. and Lygeros, J. A stochastic reach-avoid problem with random obstacles, *HSCC'11 - Proceedings of the 2011 ACM/SIGBED Hybrid Systems: Computation and Control*, 2011, pp 251–260. https://doi.org/10.1145/1967701.1967738

[79] Hupe, P., Hauf, T. and Rokitansky, C.-H. *Case Study of Adverse Weather Avoidance Modelling*, Fourth SESAR Innovation Days, 2014, November 25.

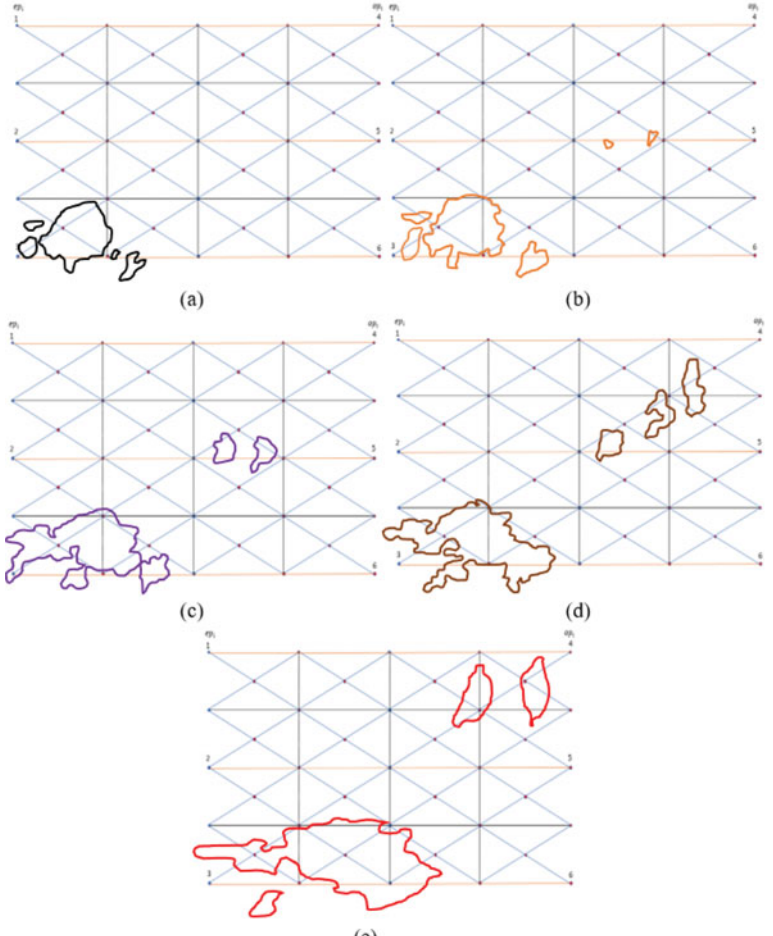
[80] Sauer, M., Sakiew, L., Hauf, T. and Hupe, P. ome applications of the adverse weather diversion model DIVMET. 16th Conference on Aviation, Range, and Aerospace Meteorology, 2013. https://www.researchgate.net/publication/305584981

Downloaded from https://www.cambridge.org/core. 17 Nov 2026 at 23:48:34, subject to the Cambridge Core terms of use.

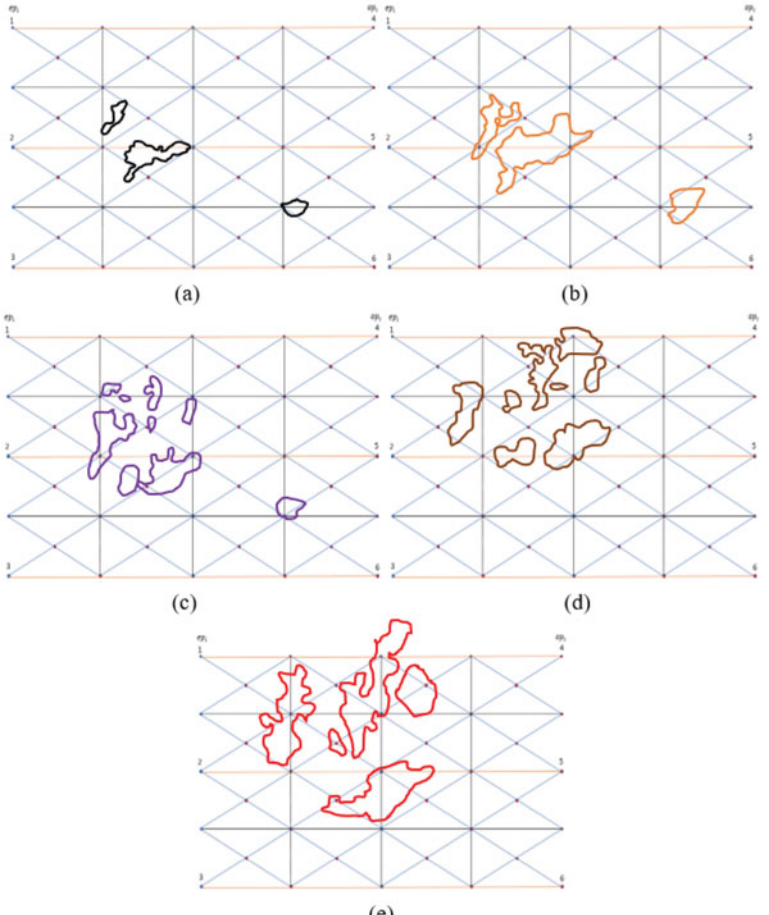
Downloaded from https://www.cambridge.org/core. 17 Nov 2026 at 23:48:34, subject to the Cambridge Core terms of use.

Appendix A. *The airspace views of convective area cases*

The airspace views for the CB-1 case



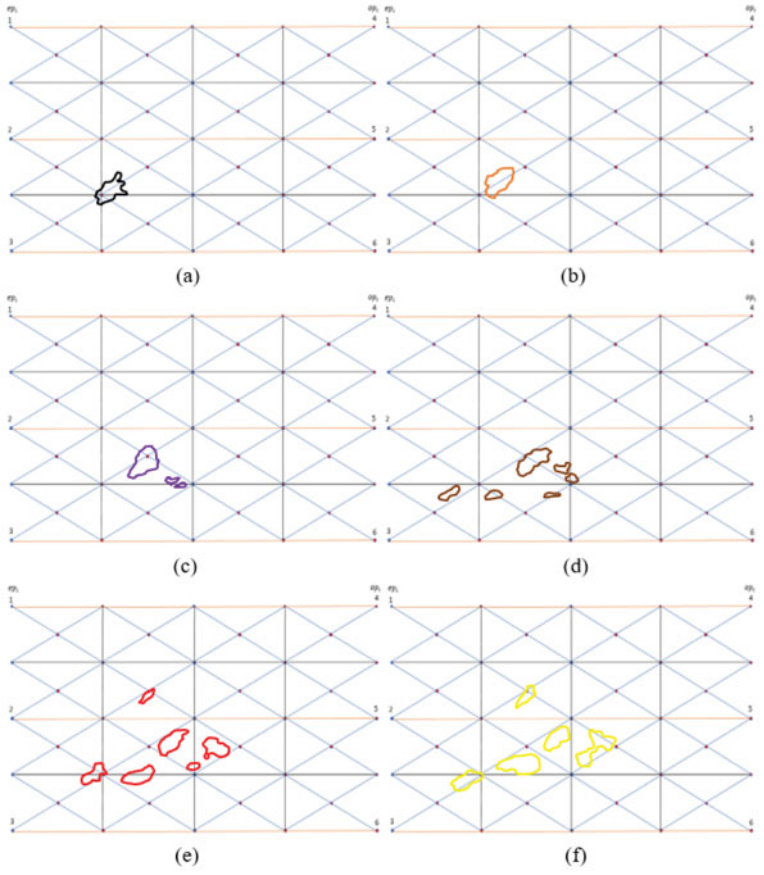
The airspace views for the CB-2 case



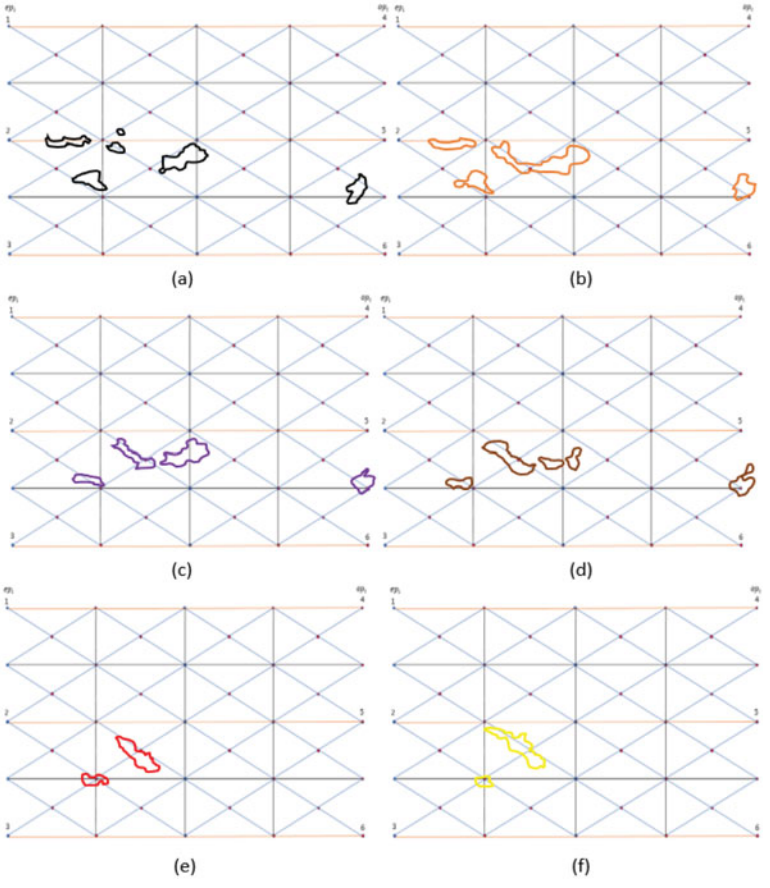
Downloaded from https://www.cambridge.org/core. 17 Nov 2026 at 23:48:34, subject to the Cambridge Core terms of use.

Appendix A *(continued).*

The airspace views for the CB-3 case



The airspace views for the CB-4 case



Appendix B. *Results of test problems in CB-1, CB-2, CB-3 and CB-4 cases*

Results of test problems in CB-1 case

Test Problem	Planning horizon	Number of aircraft	z_s	Solution time	z_v	VSS
$TP-1$	1	12	11611	50	11754	143
	2	13	13270	136	13455	185
	3	18	18177	84	18617	441
	4	20	18153	102	18680	527
	5	16	16399	227	16608	209
$TP-2$	1	6	6058	2	6058	0
	2	11	11482	38	11846	364
	3	17	18729	292	19151	422
	4	23	23475	495	- *	- **
	5	21	18254	27	18832	578
TP-3	1	12	12847	16	13118	271
	2	14	14860	69	15242	381
	3	16	15124	26	15511	387
	4	18	15578	67	15928	351
	5	15	13849	24	13951	103
TP-4	1	4	2304	1	2304	0
	2	9	8690	16	8829	138
	3	15	17970	387	- *	- **
	4	20	19910	141	20546	636
	5	22	19905	115	20534	629
TP-5	1	8	6956	3	6956	0
	2	14	15416	63	15803	387
	3	17	17939	35	18516	577
	4	20	15696	25	16194	498
	5	14	11623	12	11991	368

Results of test problems in CB-2 case

Test Problem	Planning horizon	Number of aircraft	z_s	Solution time	z_v	VSS
TP-6	1	9	9573	10	9573	0
	2	15	16710	143	16966	255
	3	18	20430	270	20699	269
	4	21	23390	201	24129	739
	5	17	18386	37	18824	438
$TP-7$	1	10	12336	8	12386	50
	2	19	21841	102	21989	148
	3	18	19740	219	19971	230
	4	20	23260	83	23983	722
	5	17	17556	97	17892	336
TP-8	1	7	9929	9	9988	58
	2	11	14632	29	14632	0
	3	16	19222	118	19579	357
	4	24	29065	342	- *	- **
	5	20	23985	328	24626	641
TP-9	1	7	7190	22	7190	0
	2	9	11617	11	11730	112
	3	15	17837	32	18292	456
	4	20	23157	42	23878	721
	5	20	25679	425	- *	- **

Downloaded from https://www.cambridge.org/core. 17 Nov 2026 at 23:48:34, subject to the Cambridge Core terms of use.

Appendix B. *(continued)*

Test Problem	Planning horizon	Number of aircraft	z_s	Solution time	z_v	VSS
$TP-10$	1	11	14916	86	15073	156
	2	13	14382	32	14741	359
	3	17	14294	70	14187	0
	4	19	23166	355	- *	- **
	5	17	24585	359	- *	- **
Results of test problems in CB-3 case						
Test Problem	Planning horizon	Number of aircraft	z_s	Solution time	z_v	VSS
TP-11	1	9	11611	8	11855	244
	2	15	15441	32	15768	327
	3	16	14312	29	14558	246
	4	20	17799	31	18360	561
	5	18	19285	113	19894	609
	6	17	16027	74	16526	499
TP-12	1	10	11597	9	11839	242
	2	10	10484	6	10814	330
	3	16	16560	27	17032	472
	4	14	15343	38	15678	335
	5	19	18897	389	- *	- **
	6	22	21102	330	- *	- **
TP-13	1	9	11065	14	11196	131
	2	16	16264	187	16404	140
	3	16	15879	84	16231	353
	4	15	16082	35	16082	0
	5	19	22133	239	22541	408
	6	19	18494	192	18844	350
TP-14	1	8	10022	9	10089	67
	2	12	12494	26	12702	208
	3	15	14076	90	14258	181
	4	14	15381	161	15516	135
	5	19	19796	372	- *	- **
	6	21	22928	397	- *	- **
TP-15	1	5	7274	5	7356	82
	2	13	15560	317	- *	- **
	3	18	16820	144	17188	368
	4	19	14776	121	15240	464
	5	19	19601	344	- *	- **
	6	19	18279	285	18611	332
Results of test problems in CB-4 case						
Test Problem	Planning horizon	Number of aircraft	z_s	Solution time	z_v	VSS
TP-16	1	6	9568	12	9761	193
	2	12	16257	303	- *	- **
	3	16	16549	87	16976	427
	4	21	18149	97	18717	568
	5	20	17011	148	17339	328
	6	20	18182	149	18756	574

Downloaded from https://www.cambridge.org/core. 17 Nov 2026 at 23:48:34, subject to the Cambridge Core terms of use.

Appendix B. *(continued)*

Test Problem	Planning horizon	Number of aircraft	z_s	Solution time	z_v	VSS
TP-17	1	8	12224	17	12502	278
	2	14	17728	302	- ∗	- ∗∗
	3	18	19641	317	- ∗	- ∗∗
	4	22	21727	212	22254	527
	5	22	20889	310	- ∗	- ∗∗
	6	17	17746	389	- ∗	- ∗∗
TP-18	1	6	9612	9	9663	51
	2	10	12164	59	12392	228
	3	16	16620	90	17037	417
	4	20	21089	164	21498	409
	5	18	16823	146	17246	423
	6	19	18031	120	18399	367
TP-19	1	9	11841	3	11841	0
	2	15	15066	73	15541	475
	3	14	11228	161	11375	147
	4	16	15025	127	15456	431
	5	17	18022	336	- ∗	- ∗∗
	6	19	19360	378	- ∗	- ∗∗
TP-20	1	7	11135	8	11233	97
	2	11	15395	312	- ∗	- ∗∗
	3	19	20020	401	- ∗	- ∗∗
	4	21	23086	319	- ∗	- ∗∗
	5	20	17444	197	19010	666
	6	19	17739	299	- ∗	- ∗∗

∗ There is no feasible solution for the problem.
∗∗ VSS could not be calculated as the z_v objective function could not be obtained

Appendix C. Additional flight trajectory examples for the CB-5 case

Figure 15 shows the flight trajectories for aircraft entering the airspace at entry point 3 and exiting at exit point 5. The pink trajectory represents the shortest feasible trajectory. To maintain the required separation, the optimisation model generates alternative trajectories through spatial conflict-resolution manoeuvres. The light blue, green and dark blue trajectories initially deviate northward to maintain conflict-free operations. By contrast, the orange trajectory follows the southern trajectory for most of the flight before performing a lateral deviation near the exit point to maintain separation while avoiding convective areas.

Figure 16 shows the flight trajectories from entry point 2 to exit point 5. Figure 16(a) shows the trajectories generated during planning horizons 1–3, where convective areas restrict traffic to a narrow southern corridor. While the green and purple trajectories merge directly into this corridor, the orange trajectory initially follows a more southerly path before merging with the main traffic flow. This additional trajectory extension provides the necessary temporal spacing to maintain the required separation within the congested corridor. Figure 16(b) shows the trajectories generated from planning horizon 4 onwards. As the convective areas in the northern part of the airspace dissipate, the optimisation model exploits the newly available airspace by assigning aircraft to shorter northern trajectories. Despite following different conflict-resolution manoeuvres, the dark blue and light blue trajectories achieve identical total flight times, with one trajectory deviating north earlier than the other. This illustrates that the proposed approach exploits newly available airspace to reduce flight times while maintaining safe separation, demonstrating its capability to improve operational efficiency under evolving weather conditions.

Downloaded from https://www.cambridge.org/core. 17 Nov 2026 at 23:48:34, subject to the Cambridge Core terms of use.

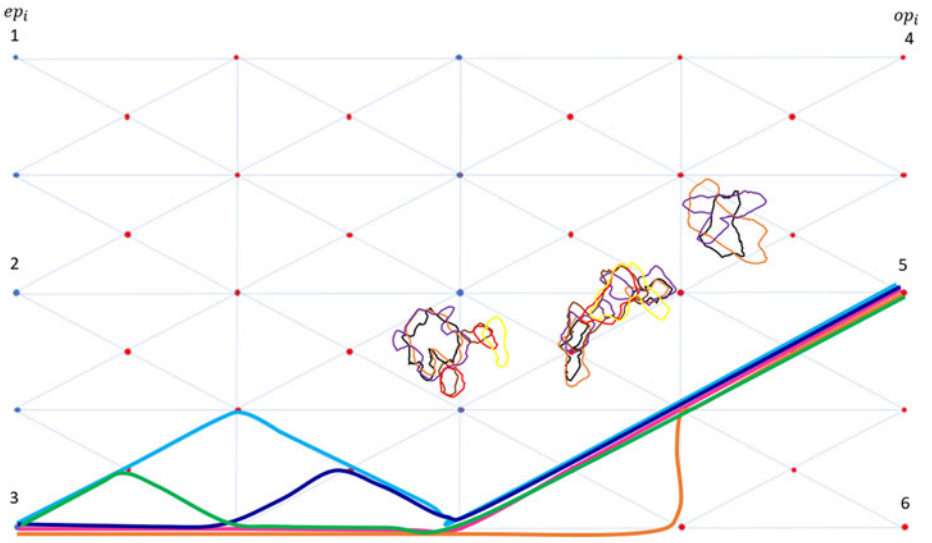


Figure 15. *Additional flight trajectories – conflict resolution.*

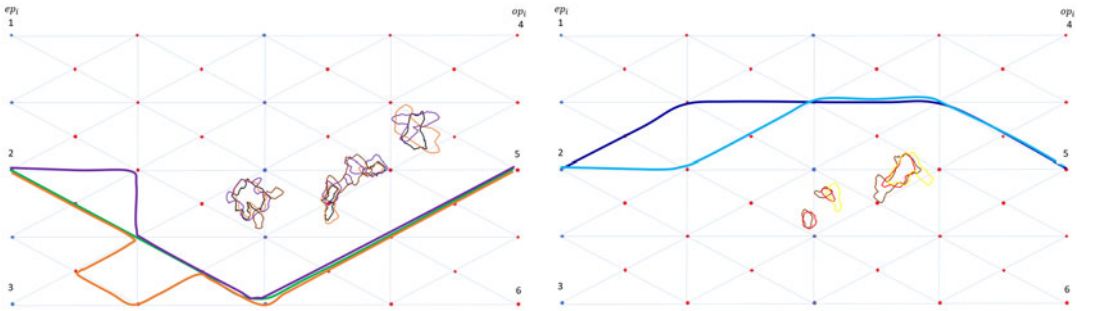


Figure 16. *Additional flight trajectories – convective weather dissipation.*

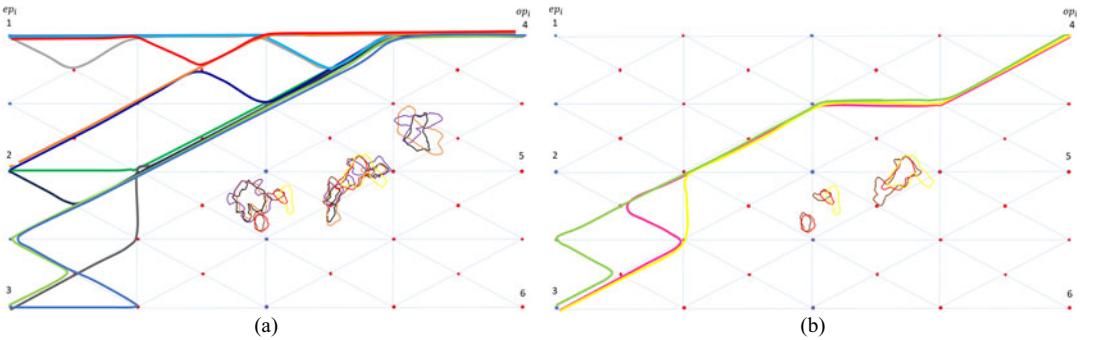


Figure 17. *Additional flight trajectories – dynamic reassignment.*

Downloaded from https://www.cambridge.org/core. 17 Nov 2026 at 23:48:34, subject to the Cambridge Core terms of use.

Figure 17 shows the flight trajectories generated for aircraft travelling from entry point 3 to exit point 4. Figure 17(a) shows that to avoid convective areas and maintain required aircraft separation, aircraft entering at entry point 3 are assigned trajectories involving lateral deviation. From planning horizon 4 onwards, additional trajectory alternatives become available, as represented by the yellow, pink and green trajectories in Figure 17(b). While the yellow trajectory is the shortest feasible option, the pink and green trajectories are re-optimised and selected at later planning horizons to resolve conflicts within the overall traffic configuration. These trajectories increase flight path lengths by introducing early lateral deviations, thereby providing the temporal spacing required to maintain conflict-free operations. This dynamic reassignment demonstrates the capability of the proposed overlapping RHC framework to adapt aircraft trajectories as convective weather conditions and traffic configurations change.

Cite this article: Kaplan Z., Çetek C. and Saraç T. Optimizing aircraft trajectories under convective weather conditions. *The Aeronautical Journal*, https://doi.org/10.1017/aer.2026.10244

Downloaded from https://www.cambridge.org/core. 17 Nov 2026 at 23:48:34, subject to the Cambridge Core terms of use.